

Water Resources Research

RESEARCH ARTICLE

10.1002/2016WR019578

Key Points:

- A parametric approach for bias correction and statistical downscaling of climate model rainfall on a user-defined high-resolution grid
- Extensive real-world comparison study of parametric and nonparametric bias correction approaches for climate model rainfall
- Parametric bias correction is more accurate and less sensitive to the calibration period, independent of the GCM/RCM combination used

Correspondence to:

A. Langousis,
andlag@alum.mit.edu.

Citation:

Mamalakos, A., A. Langousis, R. Deidda, and M. Marrocu (2017), A parametric approach for simultaneous bias correction and high-resolution downscaling of climate model rainfall, *Water Resour. Res.*, 53, 2149–2170, doi:10.1002/2016WR019578.

Received 28 JUL 2016

Accepted 25 JAN 2017

Accepted article online 3 FEB 2017

Published online 16 MAR 2017

A parametric approach for simultaneous bias correction and high-resolution downscaling of climate model rainfall

Antonios Mamalakos^{1,2}, Andreas Langousis¹ , Roberto Deidda³, and Marino Marrocu⁴
¹Department of Civil Engineering, University of Patras, Patras, Greece, ²Department of Civil and Environmental Engineering, University of California, Irvine, Irvine, California, USA, ³Dipartimento di Ingegneria Civile, Ambientale e Architettura, University of Cagliari, Cagliari, Italy, ⁴CRS4, Centro di Ricerca, Sviluppo e Studi Superiori in Sardegna, Loc. Piscina Manna, Pula, Italy

Abstract Distribution mapping has been identified as the most efficient approach to bias-correct climate model rainfall, while reproducing its statistics at spatial and temporal resolutions suitable to run hydrologic models. Yet its implementation based on empirical distributions derived from control samples (referred to as nonparametric distribution mapping) makes the method's performance sensitive to sample length variations, the presence of outliers, the spatial resolution of climate model results, and may lead to biases, especially in extreme rainfall estimation. To address these shortcomings, we propose a methodology for simultaneous bias correction and high-resolution downscaling of climate model rainfall products that uses: (a) a two-component theoretical distribution model (i.e., a generalized Pareto (GP) model for rainfall intensities above a specified threshold u^* , and an exponential model for lower rainrates), and (b) proper interpolation of the corresponding distribution parameters on a user-defined high-resolution grid, using kriging for uncertain data. We assess the performance of the suggested parametric approach relative to the nonparametric one, using daily raingauge measurements from a dense network in the island of Sardinia (Italy), and rainfall data from four GCM/RCM model chains of the ENSEMBLES project. The obtained results shed light on the competitive advantages of the parametric approach, which is proved more accurate and considerably less sensitive to the characteristics of the calibration period, independent of the GCM/RCM combination used. This is especially the case for extreme rainfall estimation, where the GP assumption allows for more accurate and robust estimates, also beyond the range of the available data.

1. Introduction

Informed societal adjustment to potential climatic changes requires in depth understanding of Earth's atmospheric response to various natural and man-made forcings, including greenhouse gas emission scenarios associated with different rates of economic and population growth [see e.g., IPCC, 2001, 2007; Vrac et al., 2007; Fowler et al., 2007; Wetterhall et al., 2009; Johnson and Sharma, 2009; Raje and Mujumdar, 2009; Palatella et al., 2010; Annan et al., 2011; Hasson et al., 2013, 2014, among others]. For the latter purpose, one needs accurate estimates of hydrological variables at a regional level and fine temporal scales (e.g., daily), suitable to run hydrologic models, and conduct impact studies [see e.g., Wilby and Harris, 2006; Perkins et al., 2007; Kjellström et al., 2010; Wilby, 2010; Evans and McCabe, 2013; Stoll et al., 2011; Teutschbein et al., 2011; Sulis et al., 2012; Deidda et al., 2013; Langousis and Kaleris, 2014; Camici et al., 2014; Piras et al., 2014, 2016; La Jeunesse et al., 2015, 2016; Dentoni et al., 2015; Majone et al., 2016; Maurer et al., 2016; Herrmann et al., 2016].

Currently, such an endeavor is possible through several open-access databases of global climate model (GCM) and regional climate model (RCM) simulations developed through projects like PCMDI/CMIP (Program for Climate Model Diagnosis and Intercomparison/Coupled Model Intercomparison Project Phases 3 and 5, <http://www.pcmdi.llnl.gov>), PRUDENCE (Prediction of Regional scenarios and Uncertainties for Defining European Climate change risks and Effects, <http://prudence.dmi.dk/>), ENSEMBLES (ENSEMBLE-based predictionS of climate change and its impacts at seasonal, decadal and centennial timescales, <http://ensembles-eu.metoffice.com>), and more recently CORDEX (COordinated Regional climate Downscaling EXperiment for regional climate change scenarios, <http://www.meteo.unican.es/en/projects/CORDEX>). Global climate models (GCMs) capture the main features of atmospheric circulation at synoptic scales (i.e., on the

order of a few degrees of latitude and longitude) [see e.g., von Storch *et al.*, 1993; Prudhomme *et al.*, 2002; Déqué, 2007; Palatella *et al.*, 2010], while RCMs improve on the GCM accuracy by resolving hydrological processes on a finer computational grid, using boundary conditions obtained from GCM simulations [see Salathé, 2003; IPCC, 2007; Fowler *et al.*, 2007; Maraun *et al.*, 2010; Teutschbein and Seibert, 2013, among others]. Hereafter, we use the abbreviation CM to refer to the combined use of GCMs and RCMs, i.e., GCM/RCM model chains.

Despite the large number of GCM/RCM simulations currently available, and the many years of research dedicated in refining models' assumptions and conceptualization, CM results still exhibit considerable biases. This is especially true in the case of rainfall, as its intermittent character and highly variable nature at hydrologically relevant spatiotemporal scales challenge modeling attempts [see e.g., Mearns *et al.*, 1995; Walsh and McGregor, 1995; Bates *et al.*, 1998; Charles *et al.*, 1999a; Prudhomme *et al.*, 2002; Busuioac *et al.*, 2006; Kiktev *et al.*, 2007; Dibikey *et al.*, 2008; Baguis *et al.*, 2009; Smiatek *et al.*, 2009; Urrutia and Vuille, 2009; Kjellström *et al.*, 2010; Willems and Vrac, 2011; Stoll *et al.*, 2011; Gagnon and Rousseau, 2013; Teutschbein and Seibert, 2013; Hasson *et al.*, 2013; Langousis and Kaleris, 2014].

Apart from the presence of biases, CM rainfall products are also characterized by intrinsic uncertainties originating from multiple sources, such as the emission scenario and initial conditions used (usually referred to as GCM intra-model variability), the length of the calibration period, the insufficient resolution of local topographic features and, more importantly, the GCM/RCM combination used [see Giorgi and Francisco, 2000; Pan *et al.*, 2001; Räisänen, 2006; Déqué *et al.*, 2007; Lucarini *et al.*, 2007; Gleckler *et al.*, 2008; Foley, 2010; Chen *et al.*, 2011; Bastola *et al.*, 2011; Sulis *et al.*, 2012; Deidda *et al.*, 2013; Hasson *et al.*, 2014; Mascaro *et al.*, 2015; Fatichi *et al.*, 2016, among others]. The latter factor (also referred to as inter-model variability) has been identified as the most critical source of uncertainty in hydrologic simulations [see e.g., Giorgi and Francisco, 2000; Déqué *et al.*, 2007; Lucarini *et al.*, 2007; Kjellström *et al.*, 2010; Chen *et al.*, 2011; Sulis *et al.*, 2012; Deidda *et al.*, 2013; Langousis *et al.*, 2016b].

The limited success of CM rainfall products in reproducing rainfall statistics (i.e., rainfall occurrence, amount, and frequency of extremes) at a basin level and at hydrologically relevant temporal scales (e.g., daily), and the increased importance of accurate precipitation estimates in determining hydrological budgets, the availability of water resources in space and time and flood risks, led to the development of statistical correction approaches (usually referred to as bias correction procedures) [see e.g., Themeßl *et al.*, 2011; Langousis *et al.*, 2016b, and references therein]. These are based on linear or more complex transformations (delta change method, power transformations, distribution mapping, etc.) [see e.g., Durman *et al.*, 2001; Kleinn *et al.*, 2005; Leander and Buishand, 2007; Déqué, 2007; Déqué *et al.*, 2007; Leander *et al.*, 2008; Michelangeli *et al.*, 2009; Sennikovs and Bethers, 2009; Piani *et al.*, 2010; Stoll *et al.*, 2011; Sun *et al.*, 2011; Rojas *et al.*, 2011; van Pelt *et al.*, 2012; Gutmann *et al.*, 2014; Mao *et al.*, 2015; Mehrotra and Sharma, 2016], with parameters estimated by comparing control runs to historical data. An implicit assumption, in all cases, is that the parameters of the transformations remain constant under time shifts [see e.g., Trenberth *et al.*, 2003; Michelangeli *et al.*, 2009; Teutschbein and Seibert, 2012, 2013] and, hence, can be used directly to bias-correct future climate projections; see e.g., the reviews in Johnson and Sharma [2011], Gudmundsson *et al.* [2012], and Teutschbein and Seibert [2012]. To that extent, several studies [Wood *et al.*, 2004; Maurer and Hidalgo, 2008; Themeßl *et al.*, 2011; Stoll *et al.*, 2011; Teutschbein and Seibert, 2012, 2013] have indicated distribution mapping (also referred to as quantile-quantile (Q-Q) correction, histogram equalization, Q-Q mapping, etc.) [see Michelangeli *et al.*, 2009; Sennikovs and Bethers, 2009; Piani *et al.*, 2010; Stoll *et al.*, 2011; Sun *et al.*, 2011; Rojas *et al.*, 2011; Sulis *et al.*, 2012, among others] as the least sensitive bias correction approach to the aforementioned implicit assumption of stationarity [Piani *et al.*, 2010; Teutschbein and Seibert, 2012, 2013] and, therefore, the most suitable one for hydrologic applications.

In its simplest form, distribution mapping is conducted by matching the quantiles of the empirical distributions obtained directly from the historical and CM data (also referred to as nonparametric distribution mapping) [see e.g., Michelangeli *et al.*, 2009; Stoll *et al.*, 2011; Themeßl *et al.*, 2011; Lafon *et al.*, 2013; Gutjahr and Heinemann, 2013], and remains sensitive to the length of the calibration period, the range of observed rainrates, and the presence of outliers [see e.g., Themeßl *et al.*, 2011; Lafon *et al.*, 2013; Langousis *et al.*, 2016b]. Another drawback of the nonparametric Q-Q correction regards regional frequency analysis of extreme rainfall, as one needs to develop separate maps of rainfall quantiles (also referred to as isohyetal maps) for each exceedance probability level (or equivalently return period) of practical interest.

In this context, several attempts have been made toward developing parametric variants of distribution mapping, where Q-Q correction is conducted based on theoretical distribution models fitted to the historical and CM simulated rainfall data [see *Piani et al.*, 2010; *Teutschbein and Seibert*, 2012; *Lafon et al.*, 2013; *Gutjahr and Heinemann*, 2013]. Contrary to the nonparametric approach, theoretical distribution models allow for more robust rainfall estimates, with approximate validity also beyond the range of the historical data [see e.g., *Langousis and Veneziano*, 2007; *Piani et al.*, 2010; *Langousis et al.*, 2013]. An additional advantage of parametric Q-Q correction, is that regional frequency analysis of extreme rainfall becomes less computationally intense, as spatial interpolation can be conducted in terms of distribution parameters, rather than empirical quantiles; see section 3.2. Note, however, that the competitive advantages of parametric Q-Q correction relative to the nonparametric one depend highly on proper selection of the theoretical distribution model, and method of fitting [see e.g., *Lafon et al.*, 2013; *Gutjahr and Heinemann*, 2013]. Unless the selected theoretical distribution model fits the data well, nonparametric approaches tend to perform better [*Gudmundsson et al.*, 2012]. Probably, this is also the reason why parametric Q-Q correction has received less attention in hydrologic applications.

Another important issue to be addressed when implementing bias correction approaches in the context of regional studies, concerns the different density and possible misalignment of observation sites and RCM grid points. While in certain cases [see e.g., *Piani et al.*, 2010; *King et al.*, 2013], this issue can be bypassed using gridded observational data (i.e., derived from station records, satellite observations, reanalysis results, and weather radar data) [see *Hofstra et al.*, 2008; *King et al.*, 2013, among others], in most cases, gridded observational data sets are not available or do not match the RCM grid. In this context, several studies [see e.g., *Vicente-Serrano et al.*, 2003; *Stahl et al.*, 2006; *Hofstra et al.*, 2008; *Moral*, 2009] have tested different approaches to interpolate rainfall measurements from surrounding locations at RCM grid points, where observational data are not available. For example, in an extended comparison study, *Hofstra et al.* [2008] applied six different interpolation methods to climate data of daily precipitation, temperature, and sea level pressure over Europe, from 1961 to 1990. The study considered angular-distance-weighting interpolation [see e.g., *Alexander et al.*, 2006; *Caesar et al.*, 2006], conditional interpolation [*Hewitson and Crane*, 2005], regression analysis [*Stahl et al.*, 2006], and two versions of kriging [see e.g., *Krige*, 1951, 1966; *Matheron*, 1971; *de Marsily*, 1986; *Kitanidis*, 1993, 1997; *Moral*, 2009; *Mazzetti and Todini*, 2009; *Furcolo et al.*, 2016]: global kriging, where a single variogram is used in the entire region, and local kriging, where a different variogram is defined for each interpolation point. The obtained results showed that global kriging performs best, while angular-distance weighting performs better when the station network is sparse.

Clearly, independent of the method used to interpolate rainfall observations on the CM grid, the resolution of the bias corrected final product is constrained by the nominal resolution of the RCM, i.e., rainfall estimates are available solely at grid points, and considered constant within each RCM grid cell. With very few exceptions of RCM simulations going down to spatial resolutions of 5 km or less [see *Gutjahr and Heinemann*, 2013; *Argüeso et al.*, 2013], typical RCM grid cells have linear dimension on the order of 0.25°–0.50° of latitude (~25–50 km) and, hence, cannot accurately resolve the statistical structure of rainfall at a basin level to conduct hydrologic impact studies [see *Laprise et al.*, 2008; *Di Luca et al.*, 2011, among others].

In an effort to address the aforementioned shortcomings, in this study, we propose a parametric bias correction procedure suited for rainfall downscaling to user-defined high spatial resolutions, and apply it to the island of Sardinia (Italy) at 1 km resolution. To do so, we: (a) fit a two-component theoretical distribution model (i.e., a generalized Pareto (GP) model for rainfall intensities above a specified threshold u^* , and an exponential model for lower rainrates) to observational and CM rainfall data, (b) use kriging for uncertain data (KUD) to spatially interpolate the distribution parameters estimated from the observational data on a user-defined high-resolution grid, and (c) use the distribution models fitted to CM data from (a) and the interpolated distribution parameters from (b), to simultaneously bias-correct and downscale CM rainfall estimates on the defined grid.

The applicability of the generalized Pareto (GP) distribution to parameterize the upper tail of the empirical distribution of rainfall has been verified both theoretically and empirically [see e.g., *Balkema and de Haan*, 1974; *Pickands*, 1975; *Leadbetter et al.*, 1983; *Smith*, 1985; *Leadbetter*, 1991; *Stedinger et al.*, 1993; *Coles*, 2001; *Martins and Stedinger*, 2001a, 2001b; *Deidda and Puliga*, 2006; *Deidda*, 2010; *Papalexiou et al.*, 2013; *Serinaldi and Kilsby*, 2014; *Langousis et al.*, 2016a]. To model low rainrates, we use an exponential distribution, as the simplest parametric form that belongs to the GP family.

To assess the performance of the suggested parametric approach relative to nonparametric distribution mapping, we use daily raingauge measurements from a dense network in the island of Sardinia (Italy), and climate model rainfall data from four CMs of the ENSEMBLES project, for the period 1951–2008, where both historical data and climate model results are available (see section 2). Calibration and validation of the parametric and nonparametric approaches is conducted using nonoverlapping time frames of different lengths, in order to avoid biasing the obtained results [see e.g., *Klemeš*, 1986; *Teutschbein and Seibert*, 2013], and also study the sensitivity of each approach to the length of the calibration period. To the best of our knowledge, this is the first time that an extensive comparison study of parametric and nonparametric approaches for bias correction of CM results is conducted on a fine resolution grid (i.e., ~ 1 km). The obtained results are promising, since the parametric approach is proved more accurate and considerably less sensitive to the characteristics of the calibration period, and the climate model used. This is especially the case for extreme rainfall estimation, where the GP assumption allows for more accurate and robust estimates, also beyond the range of the available data, allowing for improvements in hydrologic risk assessment at a regional level, based on climate model results.

In section 2, we provide some necessary information for the study region, the available data, and their use in the context of the study, and in section 3, we present details of the parametric and nonparametric approaches and their application to data. For the base case of one climate model and a single combination of calibration-validation periods (i.e., calibration: 1951–1965, validation: 1966–2008), section 4 illustrates the performance of the suggested parametric Q-Q correction procedure (i.e., relative to the nonparametric one) in reproducing the mean annual rainfall depth and extreme rainfall estimates for different exceedance probability (or equivalently return period) levels. Section 5 uses quantitative error metrics to assess the overall performance of the two approaches, and study their sensitivity to the GCM/RCM combination used and the characteristics of the calibration period. Section 6 concludes by summarizing the main findings of this study.

2. Available Data

2.1. Study Region and Observational Data

The island of Sardinia in Italy (see Figure 1a) is the second largest island in the Mediterranean Sea, with an approximate area of 24,000 km². It is located between 39° and 41° latitude (North), and 8° and 10° longitude (East). The highest mountain peak is Punta La Marmora (1834 m a.m.s.l.), which is part of the Gennargentu Range in the mainland. Sardinia has a Mediterranean climate along its coasts, plains, and low hills, with mild winters and hot summers, whereas the interior plateaus, valleys, and mountain ranges experience a continental climate with cold winters and hot summers. Rainfall exhibits a Mediterranean distribution all over the Island, with almost rainless summers and wet autumns, winters and springs. More details on the rainfall regime in Sardinia can be found in *Mascaro et al.* [2013], and references therein. Daily rainfall measurements are available at multiple locations (i.e., a total number of 424 measuring locations; see points in Figure 1a) for the period from 1922 to 2008, recorded by the raingauge network of the Hydrological Survey Agency of the Sardinia Region (<http://www.regione.sardegna.it/j/v/25?s=205270&v=2&c=5650&t=1>). Due to incompleteness of the observational time series, to establish the necessary bias correction relationships (section 3) and assess each method's performance (sections 4 and 5), we use solely those stations (i.e., a total number of 243, almost uniformly distributed over the Island; see points in Figure 1b) with more than 30 years of rainfall observations in the 58-year period from 1 January 1951 to 31 December 2008. The latter period was selected based on the availability of CM results, which starts on 1 January 1951; see section 2.2.

2.2. Climate Model Data

To study the relative performance of parametric and nonparametric distribution mapping in reproducing the statistical structure of precipitation at a daily resolution, we use climate model results (i.e., total precipitation) from four GCM/RCM combinations (i.e., KNMI, MPI, C4I, and SMHE) freely downloadable from the EU-FP6-ENSEMBLES project (<http://ensembles-eu.metoffice.com>), with available data starting on 1 January 1951. These climate model combinations have been verified and selected for hydrological modeling in several catchments in the Mediterranean region, including the island of Sardinia (Italy), in the context of the EU-FP7-CLIMB project (Climate Induced Changes on the Hydrology of Mediterranean Basins, <http://www.climb-fp7.eu>) [see *Deidda et al.*, 2013]. More precisely, MPI, KNMI, and C4I combinations use ECHAM5 (Max

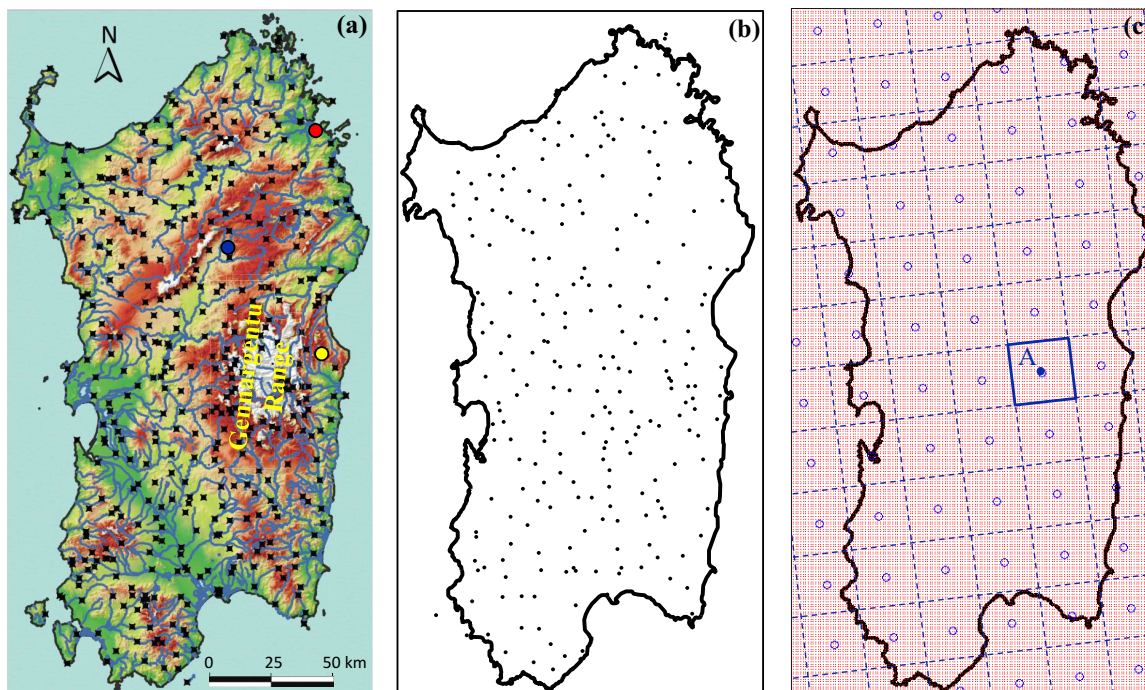


Figure 1. (a) The island of Sardinia in Italy. Points indicate rainfall measuring locations (i.e., a total number of 424), while circles indicate the stations used in Figure 2: #110 (blue), #288 (red), and #322 (yellow). (b) Spatial distribution of stations (i.e., a total number of 243) with more than 30 years of rainfall observations within the 58-year period from 1 January 1951 to 31 December 2008. (c) Grid systems over Sardinia: high-resolution grid (i.e., 1 km resolution; red dots) and climate model (CM) grid (approximately 25 km spatial resolution; blue dashed lines). Circles correspond to CM grid points at cell centres, and point A indicates the CM point used in Figure 11.

Planck Institute for Meteorology, Germany) GCM to drive the simulations of REMO (Max Planck Institute for Meteorology, Hamburg, Germany), RACMO (Royal Netherlands Meteorological Institute, Netherlands), and RCA (Swedish Meteorological and Hydrological Institute, Sweden) RCMs, respectively, while SMHE uses the outputs of HadCM3 (high sensitivity) GCM (Hadley Centre for Climate Prediction, Met Office, UK) to drive the RCA RCM simulations. The domain of integration is common to all RCMs, covering western Europe and the Mediterranean region at a resolution of approximately 25 km. To keep the paper short, in section 4, we present illustrations only for the KNMI case and a single combination of calibration-validation periods (i.e., calibration: 1951–1965, validation: 1966–2008), and in section 5, we use quantitative error metrics to thoroughly assess the overall performance of the parametric and nonparametric Q-Q correction approaches, for all models and different combinations of calibration and validation periods.

3. Methodologies

3.1. Nonparametric/Empirical Distribution Mapping

Nonparametric distribution mapping is a simple, yet powerful, approach to statistically correct CM results. The corresponding nonlinear transformation (also referred to as empirical Q-Q mapping) [see Déqué *et al.*, 2007; Teutschbein and Seibert, 2012] is obtained by matching the empirical quantiles of the historical and simulated rainfall series within a certain calibration period [see e.g., Michelangeli *et al.*, 2009; Stoll *et al.*, 2011; Themeßl *et al.*, 2011; Lafon *et al.*, 2013; Gutjahr and Heinemann, 2013]. More precisely, if $X_{CM}^{(m,k)}(t)$ is the estimate of spatially averaged rainfall inside grid cell k (see Figure 1c) on day t from climate model m , the corresponding Q-Q corrected rainfall estimate $X_{cor}^{(m,k)}(t)$ is obtained as:

$$X_{cor}^{(m,k)}(t) = F_{H,k}^{-1} \left\{ F_{m,k} \left[X_{CM}^{(m,k)}(t) \right] \right\} \quad (1)$$

where $F_{m,k}$ is the empirical cumulative distribution function (CDF) of the spatially averaged rainfall estimates of climate model m for grid cell k , and $F_{H,k}^{-1}$ is the inverse function of $F_{H,k}$; i.e., the empirical CDF of spatially averaged rainfall (using historical observations) over grid cell k . Both $F_{m,k}$ and $F_{H,k}$ are obtained using CM and observational data, respectively, for a certain calibration period and are assumed invariant to time

shifts; see Introduction. Thus, the transformation in equation (1) can be directly applied to statistically correct CM rainfall estimates within time-frames other than the calibration period (i.e., the period used to obtain $F_{m,k}$ and $F_{H,k}$).

While estimation of $F_{m,k}$ for each grid cell k and climate model m is straight forward (i.e., as CM rainfall estimates correspond to spatial averages inside each cell of the model grid), estimation of $F_{H,k}$ from observational data requires some additional effort to construct series of spatial rainfall averages from point rainfall measurements. For the latter purpose, we use simple averaging of all daily rainfall observations inside each grid cell. In case no raingauge measurements are available in the corresponding cell, we use the squared inverse distance approach [see e.g., Argüeso *et al.*, 2013; Gutjahr and Heinemann, 2013] to weight average daily rainfall measurements from the five nearest stations to the cell center.

An emerging issue when using equation (1) to bias-correct CM rainfall products, regards the case $F_{m,k}(0) > F_{H,k}(0)$. More precisely, when the marginal probability of no rain estimated from CM data exceeds that estimated from the historical record, then the minimum rainfall value produced by the transformation in equation (1) is some positive quantity different from zero. In other words, the fraction of dry days in the Q-Q corrected CM rainfall series equals zero. To bypass this problem, while preserving the fraction of dry days in the historical record also in the Q-Q corrected rainfall series, we apply the transformation below to any CM rainfall value that satisfies $x_{CM}^{(m,k)} \leq 0$ (note that CM products may include traces of numerical artifacts of negative rainfall):

$$x_{cor}^{(m,k)} = F_{H,k}^{-1}(p_k) \quad (2)$$

where p_k is uniformly distributed in the interval $[0, F_{m,k}(0)]$ (i.e., $P_k \sim U[0, F_{m,k}(0)]$).

Equations (1) and (2) are used for the nonparametric Q-Q correction of CM rainfall products over the island of Sardinia (Italy), and the obtained results are compared to those of the parametric approach described in the next section.

3.2. Parametric Distribution Mapping

The only difference between parametric distribution mapping and its empirical variant described in the previous section is that in the parametric approach $F_{m,k}$ and $F_{H,k}$ in equations (1) and (2) are not the empirical CDFs, but theoretical distribution models properly fitted to data. Suggested distributions in the literature for daily rainfall include the exponential, gamma, lognormal, and the generalized Pareto (GP) models [see e.g., Langousis and Veneziano, 2007; Piani *et al.*, 2010; Deidda, 2010; Gutjahr and Heinemann, 2013; Langousis and Kaleris, 2013; Papalexiou *et al.*, 2013; Serinaldi and Kilsby, 2014; Langousis *et al.*, 2009, 2016a], with the latter being used to model rainfall excesses above some sufficiently high threshold value u^* .

For the needs of the present study, we model daily rainfall intensities using a two-component theoretical distribution model: a GP model for rainfall intensities above a specified threshold u^* , and an exponential model for lower rainrates. Selection of a GP distribution to parameterize the upper tail of the empirical distribution of daily rainfall is based on both theoretical arguments (i.e., GP is the limiting distribution of the scaled excesses above high threshold values) [see e.g., Balkema and de Haan, 1974; Pickands, 1975; Leadbetter *et al.*, 1983; Smith, 1985; Leadbetter, 1991; Coles, 2001; Veneziano *et al.*, 2009; Veneziano and Yoon, 2013; Lucarini *et al.*, 2016] and empirical findings [see Stedinger *et al.*, 1993; Martins and Stedinger, 2001a,b; Deidda and Puliga, 2006; Deidda, 2010; Papalexiou *et al.*, 2013; Serinaldi and Kilsby, 2014; Langousis *et al.*, 2016a, among others]. To model low rainrates (i.e., below u^*), we use an exponential distribution, as the simplest parametric form that belongs to the GP family.

To fit the GP model to daily rainfall measurements and CM data in a selected calibration period, we use the multiple threshold method (MTM) developed by Deidda [2010], with a probability weighted moments (PWM) estimator [see e.g., Greenwood *et al.*, 1979; Hosking *et al.*, 1985; Hosking and Wallis, 1987, 1997; Hosking, 1990, 1992; Deidda and Puliga, 2009], hereafter referred to as MTM-PWM. MTM fits a GP model to data using a range of thresholds (rather than a single one; see below), thus, minimizing uncertainties in model parameter estimation [see Deidda, 2010; Serinaldi and Kilsby, 2014]. Fitting based on a range of possible thresholds becomes possible by proper standardization/reparameterization of the GP model to zero threshold. In this case [see Deidda, 2010]:

$$G(x) = \begin{cases} 1 - \zeta_0 \left(1 + \zeta \frac{x}{a_0}\right)^{-1/\zeta}, & \zeta \neq 0 \\ 1 - \zeta_0 \exp\left(-\frac{x}{a_0}\right), & \zeta = 0 \end{cases}, \text{ for any } x \geq 0 \quad (3)$$

where $G(x)$ is the theoretical CDF, ζ is the GP distribution shape parameter (for $\zeta = 0$, equation (3) reduces to an exponential distribution with a concentrated probability mass at zero), and

$$a_0 = a_u - \zeta u, \zeta_0 = \begin{cases} \zeta_u \left(1 + \zeta \frac{u}{a_0}\right)^{1/\zeta}, & \zeta \neq 0 \\ \zeta_u \exp\left(\frac{u}{a_0}\right), & \zeta = 0 \end{cases}, \text{ for any } u \geq 0 \quad (4)$$

where a_u is the scale parameter of the GP model when fitted to rainfall excesses above threshold u , and $\zeta_u = P[X > u]$ is the empirical probability that X exceeds u . Note that, for each selected threshold u , the parameters a_u and ζ are estimated directly from data by applying the PWM parameter estimation method to rainfall excesses above threshold u (i.e., $[X - u | X > u]$; for a detailed description of the method, the reader is referred to Hosking [1992] and Hosking and Wallis [1987, 1997]), whereas the standardized (to zero threshold) scale parameter a_0 , and the probability of rain ζ_0 , are calculated analytically using equation (4).

In the context of this study, we estimate the threshold invariant parameters a_0 , ζ and ζ_0 in equation (3) using the median of the corresponding parameter estimates obtained by fitting a GP model to the excesses above different thresholds u in the range from 2.5 to 12.5 mm/d [see Deidda, 2010]. In a few cases when the aforementioned range of threshold levels resulted in irregularly high shape parameter estimates (i.e., $\zeta \geq 0.3$), parameter estimation was repeated using higher threshold levels in the range from 6.0 to 16.0 mm. In this way, we ensure that the obtained parameter estimates are not biased by the range of the selected threshold levels. In all records analyzed, we found that above rainrates on the order of 6.5 mm/d, the GP model reproduces well the empirical CDF of daily rainfall observations and CM data. This is in accordance with the findings of Langousis et al. [2016a], where different threshold detection methods were evaluated and applied to 1700 overcentennial daily rainfall records collected worldwide. Thus, in what follows, we use threshold $u^* = 6.5$ mm/d to transition from an exponential to a GP distribution model.

To model positive rainrates below threshold $u^* = 6.5$ mm/d, we use an exponential CDF:

$$S(x) = 1 - p_0 \exp\left(-\frac{x}{b}\right), x \geq 0 \quad (5)$$

where b is the distribution scale parameter, and $1 - p_0$ is a concentrated mass at zero accounting for the fraction of dry days. Equation (5) can also be written in the form: $\log(1 - S(x)) = -x/b + \log(p_0)$. In our analysis, we use simple linear regression to estimate b as the reciprocal (i.e., inverse) of the negative slope of the log-transformed complementary CDF (i.e., $\log(1 - S(x))$) of the observational or CM data in the range (0, 6.5 mm/d). In this way, we account for all available information on low positive rainrates (i.e., below 6.5 mm/d) during distribution fitting, and calculate p_0 analytically so it ensures continuity of the two components (i.e., GP in equations (3) and (4), and exponential in equation (5)) of the distribution mixture at the point of transition, i.e., $G(u^*) = S(u^*)$. In this case:

$$p_0 = \begin{cases} \zeta_0 \exp\left[\frac{u^*}{b} - \frac{1}{\zeta} \ln\left(1 + \zeta \frac{u^*}{a_0}\right)\right], & \zeta \neq 0 \\ \zeta_0 \exp\left(\frac{u^*}{b} - \frac{u^*}{a_0}\right), & \zeta = 0 \end{cases} \quad (6)$$

Note that the alternative approach of setting p_0 to the empirical probability of rain and calculating the scale parameter b of the exponential model analytically is not recommended, due to possible quantization in the historical data (see discussion in section 4.1 and Figures 2b and 2e). Taking advantage of the threshold-invariance property of parameters ζ , a_0 , and ζ_0 (see above and Deidda [2010]), we use kriging for uncertain data (KUD) [see e.g., de Marsily, 1986; Mazzetti and Todini, 2009; Furcolo et al., 2016] to interpolate the parameters ζ , a_0 , ζ_0 , and b estimated for the selected calibration period at the locations of the raingauges

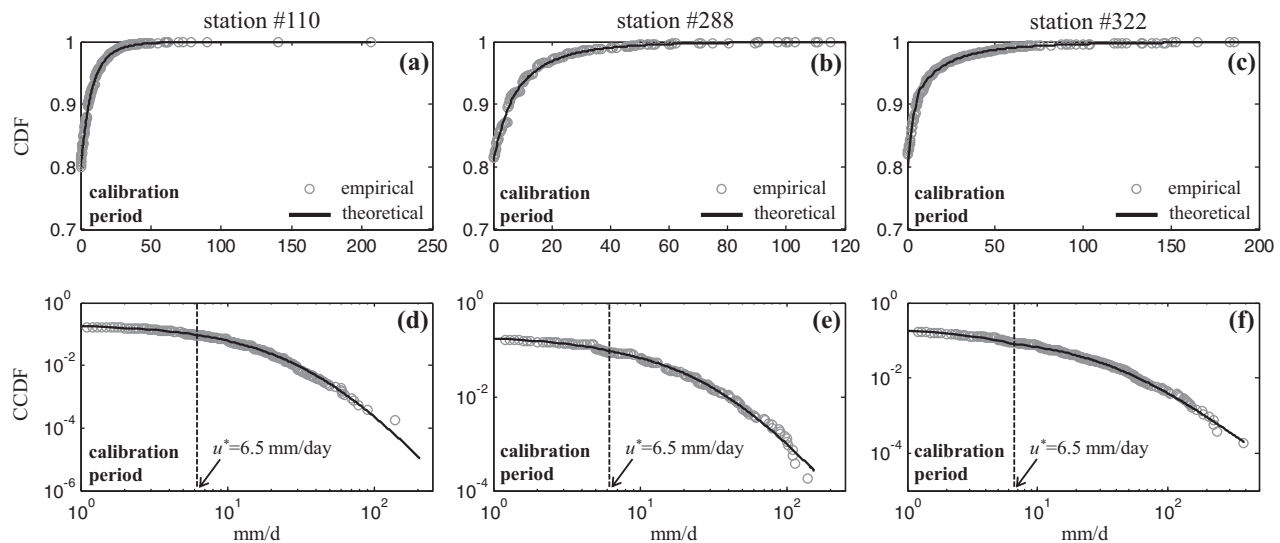


Figure 2. (top) Empirical CDFs (distribution body), (bottom) complementary CDFs (CCDFs, upper tail), and fitted theoretical distribution models (solid lines), for the three selected stations shown in Figure 1a, in the calibration period 1951–1965. Theoretical fits correspond to the two-component distribution model in equations (3–6); i.e., a GP model for rainfall intensities above threshold $u^* = 6.5$ mm/d, and an exponential model for lower rainrates.

(see points in Figure 1a), on a user-defined high-resolution grid (1 km; see red dots in Figure 1c). The parameter estimation variance at the locations of the raingauges (necessary for KUD analysis and interpolation) was obtained through Monte Carlo simulation. More precisely, at each measuring location, we used the fitted distribution mixture in equations (3–6) to simulate 1000 synthetic rainfall series for the corresponding calibration period, refitted the suggested model to each of the simulated series, and calculated the variance of the parameter estimates.

Thus, at any point l of the user-defined high-resolution grid, the theoretical CDF of historical rainfall is parameterized using the vector of interpolated parameters $[\xi^{(l)}, a_0^{(l)}, \zeta_0^{(l)}, b^{(l)}]$, and the theoretical probability of rain $p_0^{(l)}$. The latter is calculated analytically from equation (6), at each location l , as a function of the parameter vector $[\xi^{(l)}, a_0^{(l)}, \zeta_0^{(l)}, b^{(l)}]$. Under this setting, one can use equation (7) below to simultaneously bias-correct and downscale CM spatial rainfall averages over RCM grid cell k (with coarse resolution on the order of, e.g., 25–50 km), to obtain point rainfall estimates at any location l of the user-defined high-resolution grid inside the corresponding cell.

$$x_{\text{cor}}^{(m,l)}(t) = \begin{cases} Q_{\text{KUD},l}^{-1} \left\{ Q_{m,k} \left[x_{\text{CM}}^{(m,k)}(t) \right] \right\}, & x_{\text{CM}}^{(m,k)}(t) > 0 \\ Q_{\text{KUD},l}^{-1}(p_k) & , x_{\text{CM}}^{(m,k)}(t) \leq 0 \end{cases} \quad (7)$$

In equation (7), $x_{\text{CM}}^{(m,k)}(t)$ denotes the estimate of spatially averaged rainfall inside grid cell k on day t from climate model m ; $x_{\text{cor}}^{(m,l)}(t)$ is the corresponding bias-corrected and downscaled to point rainfall product at location l of the high-resolution grid; $Q_{m,k}$ denotes the theoretical CDF of the distribution mixture in equations (3–6), with parameters estimated from CM rainfall products in the coarse-resolution grid cell k ; $Q_{\text{KUD},l}$ is the CDF of the suggested distribution mixture at grid point l using the corresponding kriged parameters, and p_k is uniformly distributed in the interval $[0, Q_{m,k}(0)]$ (i.e., $P_k \sim U[0, Q_{m,k}(0)]$).

4. Results for the Base Case

In this section, we apply the nonparametric/empirical Q-Q correction (discussed in section 3.1), and the parametric approach for simultaneous bias correction and rainfall downscaling (described in section 3.2), to KNMI rainfall products. To more rigorously test the two approaches and avoid biasing the results by mixing the calibration and validation time-frames [see e.g., Klemes, 1986; Teutschbein and Seibert, 2013; Langousis et al., 2016b], we split the available data into a 15-year (1951–1965) calibration period (i.e., used to obtain model parameters) and a 43-year (1966–2008) validation period, and use the latter to assess the

performance of each method in reproducing the mean annual rainfall depth and extreme rainfall estimates for different exceedance probability (or equivalently return period) levels, by comparing to historical observations.

4.1. Calibration of the Parametric Approach: Distribution Fitting and KUD Interpolation

Figure 2 shows the empirical and theoretical (i.e., the two-component distribution model in equations (3–6)) CDFs and complementary CDFs (CCDFs) for three indicative stations (i.e., #110, #288, and #322; see colored circles in Figure 1a), in the calibration period 1951–1965. In all three cases, the distribution mixture fitted using the MTM-PWM method for the GP upper part of the distribution (i.e., above threshold $u^* = 6.5$ mm/d), and equation (6) for the exponential lower part, approximates the data well, even in cases of high quantization levels (see Figures 2b and 2e). This is an important attribute of the MTM method, as common approaches to fit a GP distribution model to data are sensitive to the level of data quantization [see Deidda and Puliga, 2006, 2009; Deidda, 2010; Langousis et al., 2016a]. Similarly, good fits have been obtained for all stations and calibration periods analyzed (not shown here for brevity).

To determine the optimum number of the closest measuring locations/stations to condition KUD interpolation, we implemented the following cross-validation procedure: (1) At each measuring location, we neglected the local recordings, and estimated the corresponding distribution parameters by conditioning KUD on the closest n ($n = 1, 2, \dots, 50$) stations. (2) For each measuring location and different number of stations n , we calculated the estimation error e relative to the parameter values obtained by fitting the distribution model directly to the local time series using MTM-PWM. (3) For each parameter, we calculated the mean absolute error, and error variance ratio, over all measuring locations, as a function of the number of stations n used to condition KUD.

Figure 3 shows results for the mean absolute error (Figure 3a, left) and error variance ratio ($\text{Var}[e]/\text{Var}[\xi]$, Figure 3b, right) of GP shape parameter estimates using KUD, as obtained using daily rainfall measurements in the 15-year calibration period 1951–1965. Clearly, small values of n (i.e., $n < 5$) lead to increased estimation variance, whereas values of $n > 12$ increase the computational time without improving the estimation accuracy. As illustrated in both Figures 3a and 3b, the number of stations that minimizes uncertainties in KUD estimates is $n = 10$, with negligible overall bias $E[e] = 10^{-4}$ (not shown in the plots). Similar results have been obtained for the remaining distribution parameters and different 15-year calibration periods. Hence, in what follows, we use the closest $n = 10$ stations to condition KUD estimation of distribution parameters on the user-defined high-resolution grid.

Figure 4 shows the empirical semivariograms of parameters ξ , a_0 , ζ_0 , and b of the two-component distribution model in equations (3–6), as obtained from daily rainfall measurements in the calibration period 1951–1965, assuming a single semivariogram function for the whole study region (see Hofstra et al. [2008] and section 1). Dashed lines correspond to least square fits of the best performing theoretical semivariogram models used for interpolation. Options tested include the Gauss, Exponential, Hole-effect, Power, Linear, and Log models [see e.g., Cressie, 1985; de Marsily, 1986; Kitanidis, 1993, 1997]. One sees that all four

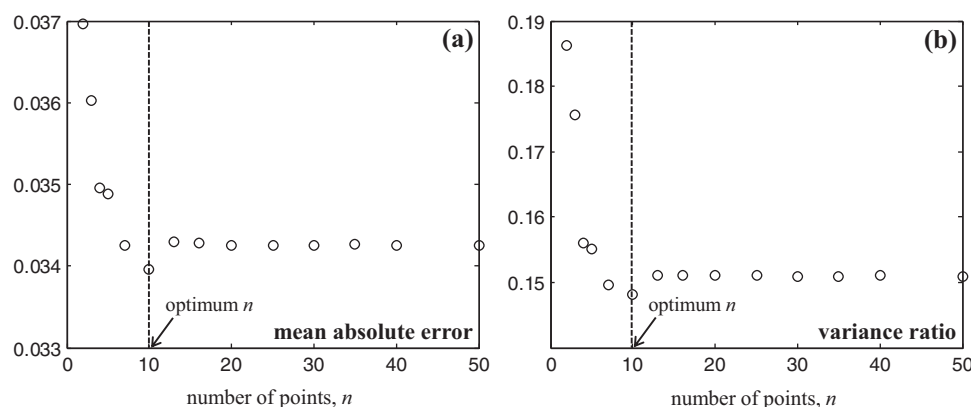


Figure 3. (a) Mean absolute error of ξ estimates, as a function of the number of points n used for KUD interpolation. (b) Same as Figure 3a but for the error variance ratio $\text{Var}[e]/\text{Var}[\xi]$; see main text for details.

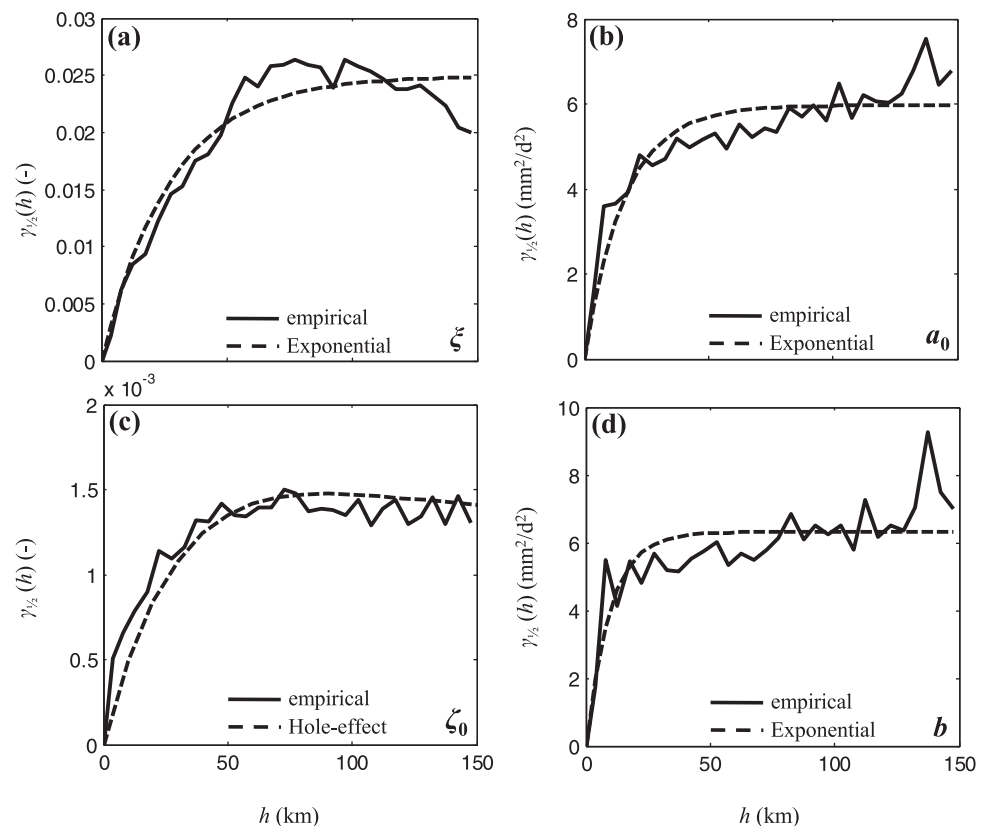


Figure 4. Empirical (i.e., calibration period 1951–1965; solid lines) and theoretical (dashed lines) semivariograms $\gamma_{1/2}(h)$, where h denotes the inter-station distance, for the parameters of the two-component theoretical distribution model in equations (3)–(6): (a) ζ_0 , (b) a_0 , (c) ζ_0 , and (d) b .

parameters exhibit a typical spatial correlation structure, with nearby locations (i.e., small values of the inter-station distance h) exhibiting high levels of dependence, and distant locations (i.e., large values of h) being almost uncorrelated (i.e., the semivariogram function reaches a sill, corresponding to the large-scale variance of the parameter over the study region). The rate of decrease of spatial correlation with the inter-station distance h varies among parameters, with the corresponding estimates becoming uncorrelated when the inter-station distance h exceeds a critical length scale h_c on the order of 20–100 km. The latter range is in accordance with the characteristic temporal and spatial scales of rainfall generating features that dominate precipitation occurrence and amount [see e.g., Veneziano and Langousis, 2005; Koutsoyiannis and Langousis, 2011; Langousis and Kaleris, 2013]. More precisely, daily precipitation in regions with Mediterranean climate is dominated by moderate to large mesoscale (i.e., linear scales on the order of 20–100 km) and synoptic scale systems (i.e., linear scales > 100 km), with lifetimes from several hours to more than a day [see Langousis and Kaleris, 2013, Table 8].

Figure 5 illustrates contour maps of the krigged parameters ζ , a_0 , ζ_0 , and b at 1 km spatial resolution, and Figure 6 shows the spatial variation of the empirically estimated and theoretically calculated (i.e., through equation (6)) fraction of wet days p_0 over Sardinia. Evidently, the west part of the Island is drier than the east part, with lower probability of rain (see Figures 5c, 6a, and 6b). Precipitation is more intense on the eastern side of the Gennargentu Range (as indicated by the high GP shape parameter values in Figure 5a), as moist air masses from the sea move upslope and cool causing precipitation to form (i.e., orographic lifting, see e.g., Singh [1992], Smith [1993], and Koutsoyiannis and Langousis [2011]). Two additional notes to make are that: (a) while both ζ_0 (i.e., the theoretical probability of rain in equation (3); see Figure 5c) and p_0 (the theoretical probability of rain in equation (6); see Figure 6b) capture the general tendency of different regions of the Island to be either wet or dry, ζ_0 cannot accurately resolve small-scale variations. This finding highlights the necessity of modeling the frequency of low (i.e., < 6.5 mm/d) and zero rainfall intensities using the exponential model in equation (5). (b) While both empirical (Figure 6a) and theoretical (Figure 6b)

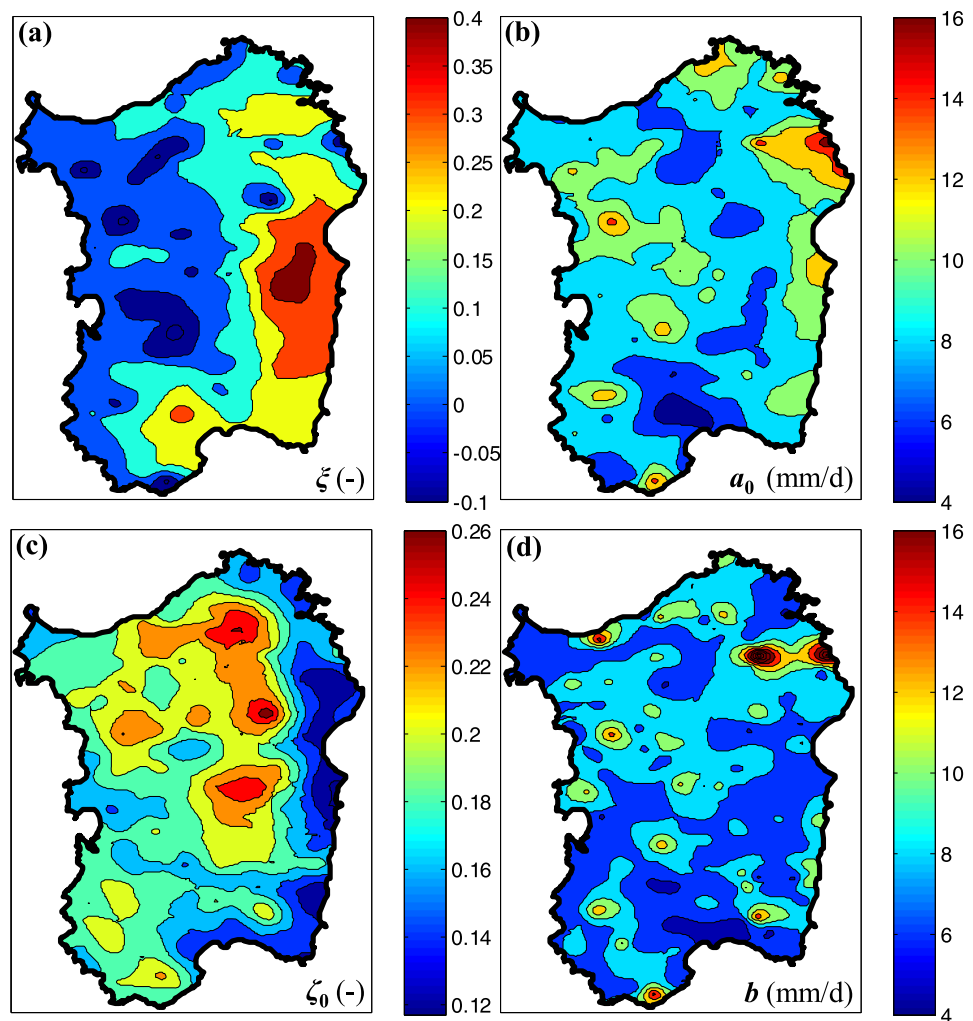


Figure 5. Contour maps for the parameters of the two-component theoretical distribution model in the calibration period 1951–1965, interpolated using kriging for uncertain data (KUD): (a) GP shape parameter ξ , (b) standardized to zero threshold scale parameter a_0 (mm/d), (c) theoretical probability of rain ζ_0 , and (d) scale parameter b (mm/d) of the exponential distribution in equation (5).

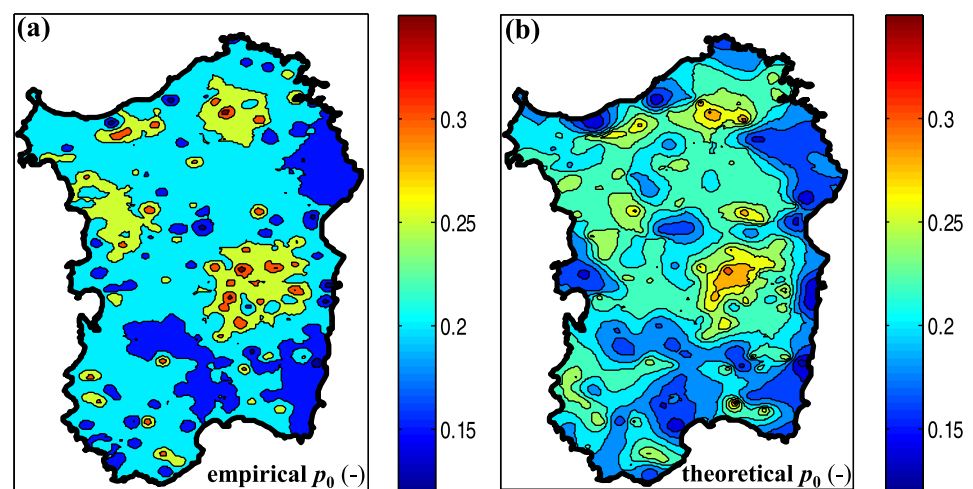


Figure 6. Spatial variation of the empirically estimated and theoretically calculated (i.e., through equation (6)) fraction of wet days p_0 over Sardinia.

estimates of the wet-day fraction display similar patterns of spatial variation, empirical estimates are more intermittent. The latter is mainly due to the various levels of data quantization at different parts of the Island, caused during data collection (i.e., different instrumentation types) and processing (e.g., dew and fog drip, also referred to as occult precipitation, artificially increase the fraction of rainy days in forested areas of the Island). This is exactly the reason why we skipped using empirical estimates of wet-day fraction, and fitted the exponential distribution model in equation (5) by estimating the scale parameter b using all available information on low positive rainrates (i.e., below 6.5 mm/d); see discussion on equation (5) in section 3.2.

4.2. Comparison Between Parametric and Nonparametric Approaches

Figure 7 illustrates the spatial distribution of the mean annual rainfall depth (mm/yr) in Sardinia for the 43-year validation period from 1966 to 2008, as obtained from: (a) the historical record of daily rainfall measurements, (b) raw KNMI rainfall estimates, (c) bias-corrected KNMI rainfall products using nonparametric distribution mapping (see section 3.1), and (d) Q-Q corrected KNMI rainfall products using the parametric approach described in section 3.2. A first observation one makes is that, on average, raw KNMI rainfall estimates (see Figure 7b) significantly underestimate the actual rainfall accumulation in Sardinia (see Figure 7a), while exhibiting reduced skill in capturing the spatial distribution of mean annual rainfall (compare Figure 7b with 7a). For example, the maximum annual rainfall depth estimated by KNMI is on the order of 900 mm/yr on the west side of Gennargentu Range, whereas the available data indicate a maximum value

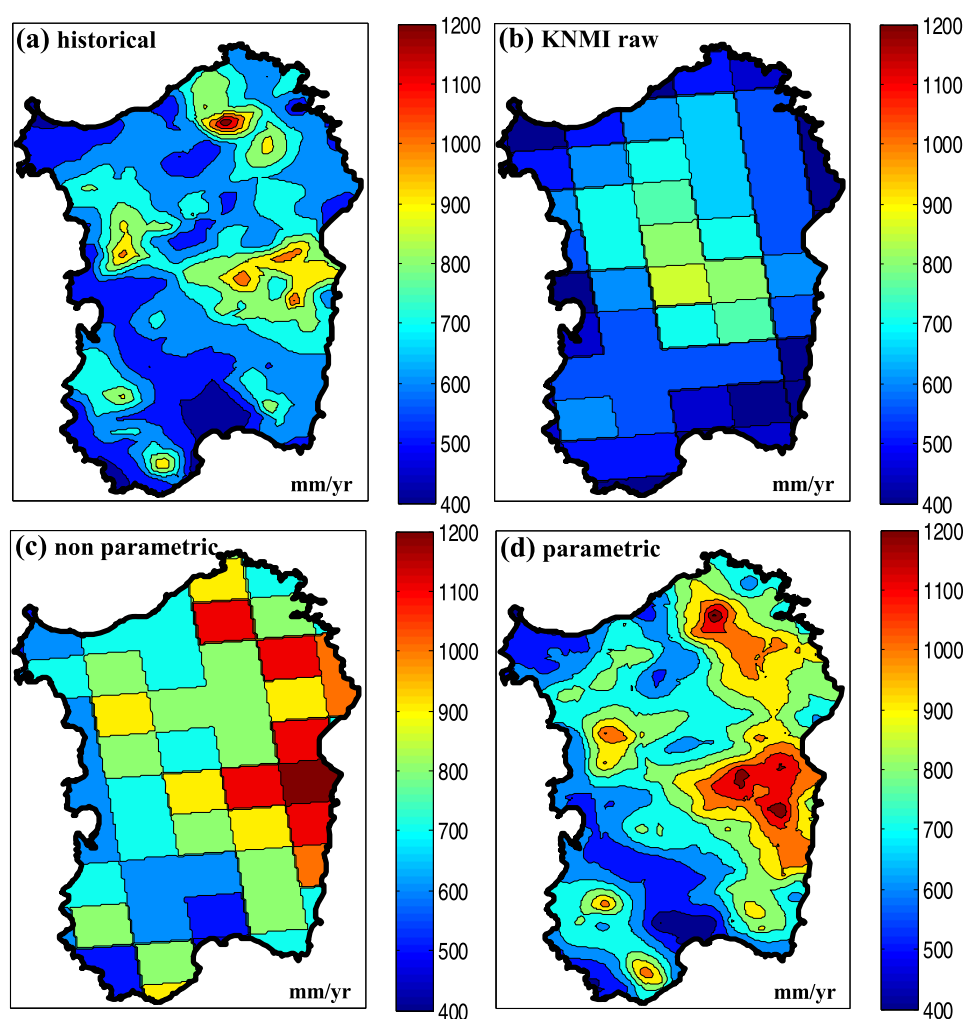


Figure 7. Estimates of the mean annual rainfall depth (mm/yr) for the 43-year validation period 1966–2008, using: (a) historical rainfall observations, (b) KNMI raw rainfall products, (c) bias-corrected KNMI products using nonparametric distribution mapping, and (d) bias-corrected KNMI rainfall products using parametric distribution mapping, with parameters drawn from Figure 5.

close to 1200 mm/yr on the east side of the mountain range. This difference can be attributed to the low resolution of the RCM computational grid (i.e., on the order of 25 km; see section 2.2), and the fact that CM rainfall estimates correspond to spatial rainfall averages (i.e., over grid cells), rather than to point rainfall estimates.

Concerning the two Q-Q correction approaches (nonparametric: Figure 7c, and parametric: Figure 7d), it is clear that they both improve on KNMI results (Figure 7b). However, detailed comparison of Figures 7c and 7d with Figure 7a reveals that the parametric approach is more accurate in reproducing the effects of topography and local climate (see discussion in section 4.1) on the fine-scale spatial structure of annual rainfall accumulations. This is especially the case at the north-east coastal part of the Island, where the nonparametric approach produces rainfall estimates in the range 1000–1200 mm/yr, whereas both historical observations and the parametrically Q-Q corrected CM results point to much lower rainfall depths.

Shifting to extreme rainfall estimation, Figures 8 and 9 show contour maps of the $T = 5$ -year and $T = 10$ -year return period rainfall intensity values (i.e., $T = 1 \text{ year}/(1 - p^{365})$, where p denotes the nonexceedance probability and 365 is the number of days in a year) [see e.g., Veneziano *et al.*, 2007; Deidda, 2010], respectively, as obtained from historical observations, raw KNMI rainfall products, and Q-Q corrected CM results using the two bias correction approaches described in sections 3.1 and 3.2. Clearly, raw KNMI rainfall products considerably underestimate extreme rainfall (compare Figures 8b and 9b with Figures 8a and 9a), especially at the east coast. An additional observation one makes is that the parametric approach reproduces

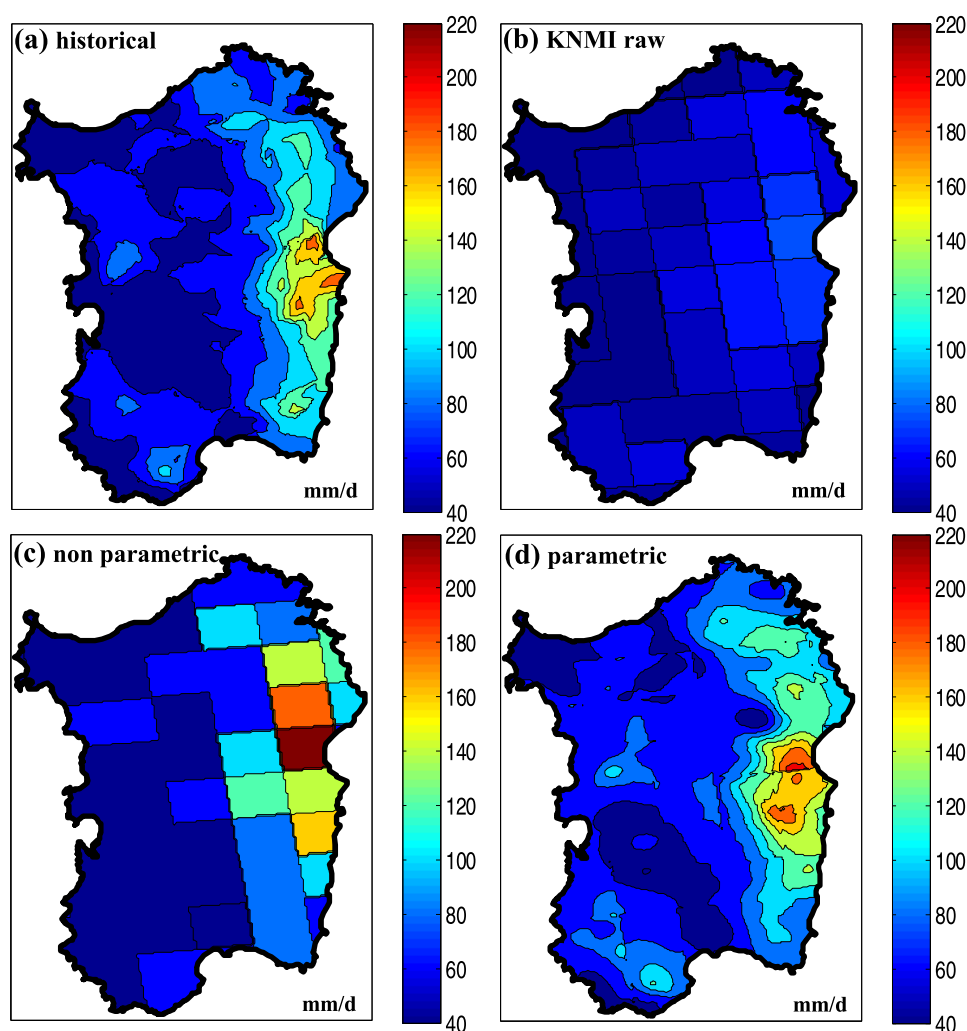


Figure 8. Same as Figure 7, but for rainfall intensity estimates (mm/d) at return period level $T = 5$ years.

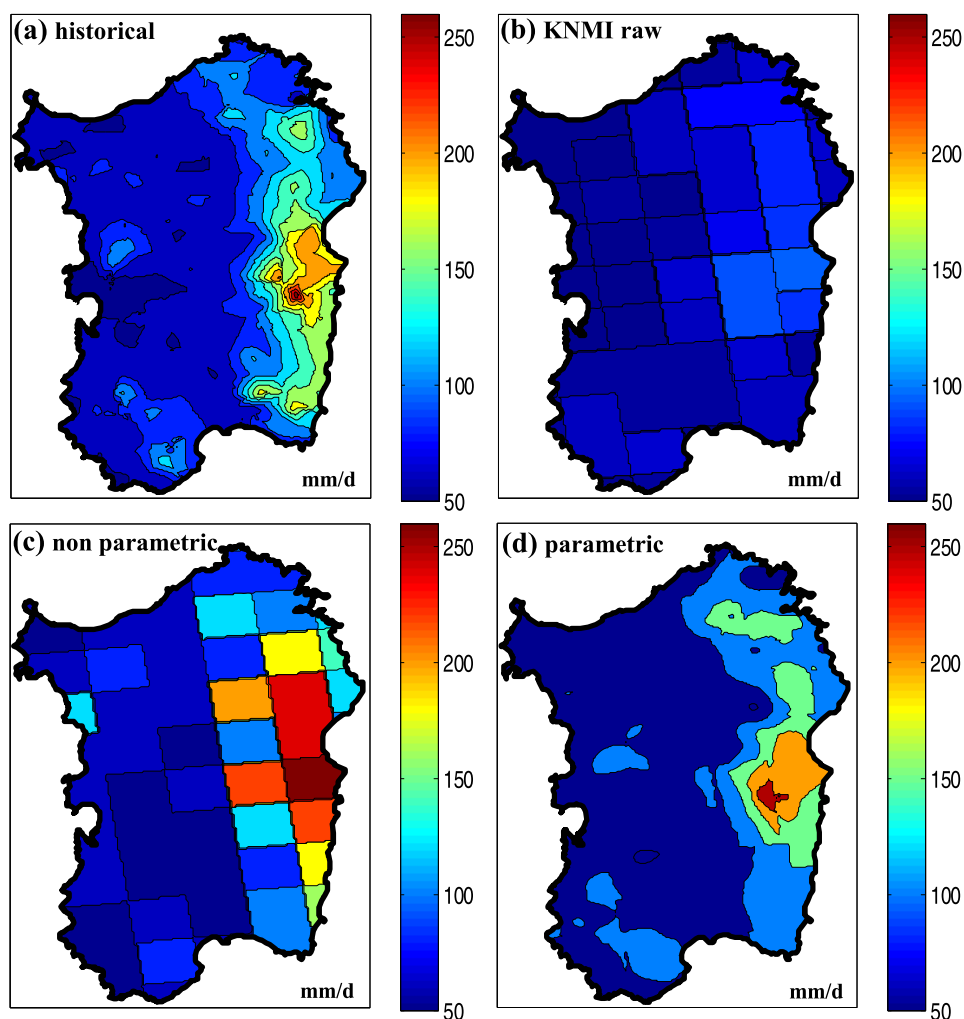


Figure 9. Same as Figure 7, but for rainfall intensity estimates (mm/d) at return period level $T = 10$ years.

well both the magnitude and spatial distribution of empirical rainfall intensity estimates (compare Figures 8d and 9d with Figures 8a and 9a), whereas the nonparametric approach overestimates extreme rainfall at the east coast of the Island (compare Figures 8c and 9c with Figures 8a and 9a). The increased accuracy of the parametric approach in modeling extreme rainfall should be attributed to: (a) the use of a GP distribution to describe the upper tail of empirical rainrates, which makes Q-Q correction rather insensitive to the characteristics of the calibration period (including its length), allowing for more robust estimates, and (b) the quality of the parametric fits of the two-component distribution mixture in the calibration period 1951–1965; see Figure 2 and discussion in section 4.1.

Overall, while neither approach can perfectly reproduce the historical rainfall statistics in the validation period based on CM data, the parametric approach proves more efficient in modeling the effects of topography and local climatology on the magnitude, general tendencies and high-resolution spatial structure of rainfall statistics, including extremes. This is an important attribute of the suggested parametric Q-Q correction procedure, which allows for improved assessment of hydrologic risks and water management practices, based on climate model results.

5. Sensitivity to Calibration-Validation Periods and the Climate Model Used

In this section, we study the sensitivity of the proposed approach to different combinations of calibration-validation periods, and climate models. Due to space limitations, and in order to quantitatively assess the

Table 1. Dimensionless RMSEs (%) for Different Combinations of Calibration-Validation Periods, Based on Q-Q Corrected KNMI Rainfall Products Using Nonparametric (i.e., Empirical; emp.) and Parametric (par.) Distribution Mapping^a

Calibration Period	Validation Period	Mean Annual Depth		T = 2 years		T = 5 years		T = 10 years		T = 30 years	
		emp.	par.	emp.	par.	emp.	par.	emp.	par.	emp.	par.
1951–1980	1981–2008	33.19	24.46	19.14	19.02	21.36	19.00	35.45	21.30	31.90	25.02
1951–1965		39.09	30.15	18.91	25.09	27.29	24.61	44.08	26.54	36.84	28.96
1951–1957		37.63	25.98	27.13	27.83	38.44	26.21	49.22	29.83	40.84	31.17
1951–1965	1966–2008	29.37	19.96	16.91	19.15	26.02	17.64	40.97	21.49	34.79	25.03
1951–1957		29.98	20.56	23.95	22.47	37.24	21.54	46.54	24.20	37.40	28.72
1981–2008	1951–1980	23.89	28.22	25.71	16.77	28.84	21.11	30.49	23.61	37.02	27.39

^aBold values indicate cases where the nonparametric approach performs better.

relative performance of the parametric and nonparametric approaches, we apply the dimensionless error metric in equation (8), hereafter referred to as DRMSE (dimensionless root mean square error), to all points of the user-defined high-resolution grid (see red dots in Figure 1c and discussion in section 3.2):

$$DRMSE = \left(\frac{1}{N} \sum_{i=1}^N \left(\frac{z_i' - z_i}{z_i} \right)^2 \right)^{1/2} \quad (8)$$

where N is the total number of grid points, and z_i and z_i' are historical and model-based estimates of statistic Z at grid point i , respectively.

Table 1 presents DRMSE values for different combinations of calibration-validation periods, based on Q-Q corrected KNMI rainfall products using empirical and parametric distribution mapping. With the exception of 4 out of the 30 cases considered (i.e., combinations of calibration-validation periods, and statistics used), the parametric approach produces lower DRMSEs. Note that the aforementioned exceptions (see bold values in Table 1) are associated with low nonexceedance probability levels (i.e., mean annual rainfall depth, and rainfall intensities for return periods $T \leq 2$ years), where the parametric fits of the suggested theoretical distribution mixture may deviate somewhat from the empirical histograms. However, for low exceedance probability levels (i.e., return periods $T > 2$ years), the performance of the parametric approach is always better.

The sensitivity of parametric and nonparametric distribution mapping to the length of the calibration period is obtained by direct comparison of DRMSEs for the same validation (i.e., column 2 in Table 1) and different calibration periods (i.e., column 1 in Table 1). As expected, the performance of the nonparametric approach decreases fast as the length of the calibration period decreases, or the return period T increases; see e.g., DRMSEs for the case when calibration is conducted using 7 years of historical data (i.e., 1951–1957). The results are much more satisfactory for the parametric approach, with the accuracy of the method being less sensitive to the length of the calibration period, and the corresponding DRMSEs increasing at a slower rate with increasing return period T . Very similar findings, favoring the parametric approach (see Table 2), were obtained also in the case when equation (8) was applied after up-scaling (i.e., through spatial averaging of daily estimates) the parametrically corrected high-resolution rainfall intensity field, to the CM grid

Table 2. Same as Table 1, But After Up-Scaling (i.e., Through Spatial Averaging of Daily Rainfall Estimates) the Parametrically Corrected High-Resolution Rainfall Intensity Field, to the CM Grid

Calibration Period	Validation Period	Mean Annual Depth		T = 2 years		T = 5 years		T = 10 years		T = 30 years	
		emp.	par.	emp.	par.	emp.	par.	emp.	par.	emp.	par.
1951–1980	1981–2008	33.19	26.00	19.14	21.41	21.36	21.15	35.45	25.31	31.90	28.43
1951–1965		39.09	31.11	18.91	26.79	27.29	26.03	44.08	29.65	36.84	31.21
1951–1957		37.63	26.14	27.13	29.42	38.44	27.72	49.22	33.78	40.84	34.64
1951–1965	1966–2008	29.37	21.49	16.91	21.27	26.02	19.71	40.97	24.41	34.79	27.06
1951–1957		29.98	20.84	23.95	24.24	37.24	23.39	46.54	27.84	37.40	31.51
1981–2008	1951–1980	23.89	28.88	25.71	17.95	28.84	21.81	30.49	24.32	37.02	28.04

Table 3. Same as Table 1, But After Randomly Eliminating Half of the Station Records Used

Calibration Period	Validation Period	Mean Annual Depth		$T = 2$ years		$T = 5$ years		$T = 10$ years		$T = 30$ years	
		emp.	par.	emp.	par.	emp.	par.	emp.	par.	emp.	par.
1951–1980	1981–2008	34.04	23.94	21.36	18.70	21.61	18.00	31.47	18.95	33.27	25.09
1951–1965		40.09	30.66	24.78	23.34	32.16	21.82	41.97	25.87	34.44	27.07
1951–1957		40.55	24.93	31.81	27.00	49.13	23.45	50.53	27.36	40.18	34.54
1951–1965	1966–2008	30.65	21.61	21.22	19.47	29.93	18.29	36.02	21.62	35.60	26.69
1951–1957		33.71	20.06	28.30	19.98	44.31	18.30	44.42	20.90	37.28	25.98
1981–2008	1951–1980	25.69	28.00	24.45	18.14	26.61	21.92	29.71	25.17	36.07	29.13

(i.e., approximate resolution of 25 km). This finding indicates that the improved performance of parametric Q-Q mapping relative to its empirical variant is also due to improvements in bias correction, and does not originate solely from KUD interpolation of distribution parameters.

To explore the sensitivity of the performance of each method to the density of the raingauge network, Table 3 shows DRMSE values obtained by applying the parametric and nonparametric approaches after randomly eliminating half of the stations in the study region; i.e., maintaining only 121 stations. One sees that the efficiency of the parametric approach, relative to the nonparametric one, is even better, with the nonparametric approach producing slightly better results in only one out of the 30 cases studied (i.e., when all stations are included in the analysis, the nonparametric approach produces better results in 4 out of 30 cases; see Table 1 and discussion above). This should be attributed to the robustness of KUD interpolation of model parameters, which makes the obtained results less sensitive to the density of the raingauge network, relative to the nonparametric approach. An additional note to be made here is that, due to the increase of statistical variability caused by the reduction of the station density, the values in Tables 1 and 3 are not directly comparable. This explains why the values in Table 3 are either slightly smaller or larger than the corresponding ones in Table 1.

To study the sensitivity of the two approaches on the CM used, for the statistics in Table 1 and three combinations of calibration-validation periods, Figure 10 shows the DRMSEs obtained when applying the nonparametric (DRMSE_n , Figure 10a) and parametric (DRMSE_p , Figure 10b) bias correction approaches to four different CMs (i.e., KNMI: green, MPI: red, C4I: blue, and SMHE: magenta), as well as the difference $\delta = \text{DRMSE}_n - \text{DRMSE}_p$ (Figure 10c). Positive values of δ indicate superiority of the parametric approach. One sees that, independent of the climate model used and the combination of calibration-validation periods, the parametric approach is on average slightly more accurate in reproducing the mean annual rainfall, but its efficiency increases fast as the exceedance probability level influencing the corresponding statistics decreases (see e.g., DRMSEs and δ associated with rainfall quantiles for $T = 2, 5, 10$, and 30 years). In addition, the reduced spread of the points in Figure 10b relative to Figure 10a, indicates the increased robustness of the parametric approach (i.e., relative to the nonparametric one) to the climate model used.

An exception occurs for the $T = 30$ -year rainfall intensity estimates of model C4I (see encompassed points in Figures 10b and 10c), where the nonparametric approach produces more accurate results independent of the calibration-validation periods used. We have investigated this issue in more detail, and found that it is due to significant differences in the body and upper tail of the empirical distributions of C4I raw rainfall estimates and those based on observations, in the region of Gennargentu Range. To illustrate this, Figure 11 compares: (i) the empirical (circles) and theoretical (solid line) CCDFs at point A in Figure 1c, obtained using C4I raw rainfall products, and ii) the CCDF of spatially averaged rainfall over the corresponding grid cell (squares), as obtained from raingauge measurements. Note in particular the good fit of the two-component distribution mixture to CM rainfall products, as well as the considerable difference in the upper tail of CM and historical rainfall data. The latter is also revealed when comparing the GP shape parameter estimates obtained using MTM-PWM; i.e., $\xi = 0.07$ (C4I), and 0.35 (historical). Notably, the incapacity of C4I rainfall products in reproducing the upper tail behavior of historical estimates, causes significant overestimation of rainfall values at high return period (i.e., low exceedance probability) levels; i.e., when parametrically corrected/transformed, small differences in C4I rainfall estimates amplify considerably. This is not the case for nonparametric approaches in general, where the empirical CDF is artificially upper bounded by the largest rainfall intensity value in the calibration period.

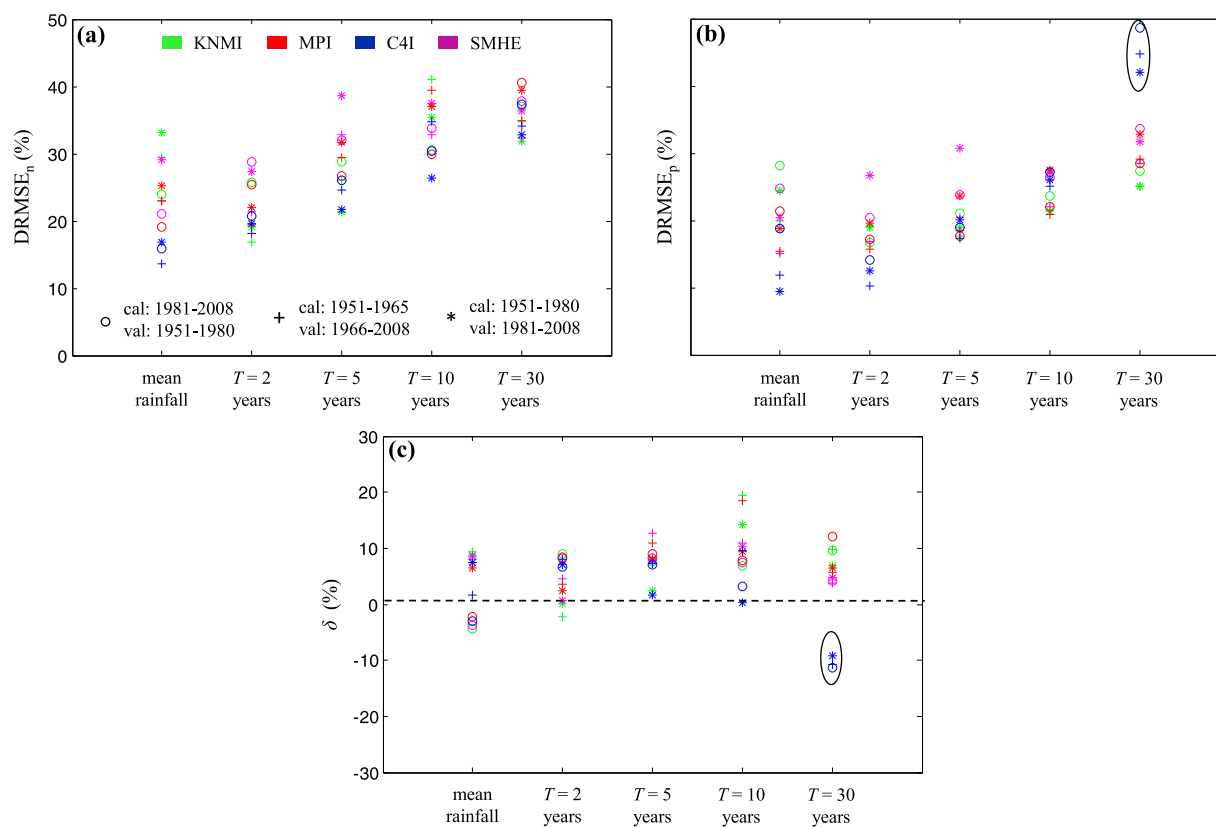


Figure 10. (a) Dimensionless RMSEs (%) for the statistics in Table 1, obtained by applying the nonparametric bias correction approach (DRMSE_n) to four different CMs (i.e., KNMI: green, MPI: red, C4I: blue, and SMHE: magenta), for three combinations of nonoverlapping calibration-validation periods. (b) Same as Figure 10a, but for the case of parametric distribution mapping (DRMSE_p). (c) Same as Figure 10a but for the difference $\delta = \text{DRMSE}_n - \text{DRMSE}_p$. Positive values of δ indicate superiority of the parametric approach.

Evidently, while parametric bias correction of climate model results: (a) demonstrates significant skill in modeling the effects of topography and local climatology on the magnitude, general tendencies, and high-resolution spatial structure of rainfall statistics, including rainfall extremes, and (b) it is rather insensitive to the characteristics of the calibration period, including its length, and the climate model used; still it cannot eliminate the signature of pronounced biases in raw CM rainfall products. Consequently, selection of the best performing GCM/RCM combination for the region of interest remains an important step prior to any

hydroclimatic impact study [see e.g., Räisänen, 2006; Perkins et al., 2007; Lucarini et al., 2007; Wilby, 2010; Sulis et al., 2012; Deidda et al., 2013].

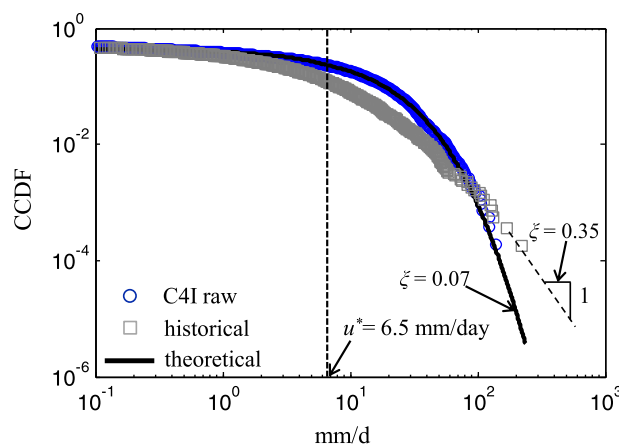


Figure 11. Empirical complementary CDFs (CCDFs, upper tail; calibration period 1951–1965) and theoretical distribution model fitted to C4I raw rainfall products (circles), and historical data (squares).

6. Conclusions

Due to its intermittent and highly variable character, and the modeling parameterizations used, rainfall is one of the least well-reproduced variables by both global climate models (GCMs) and regional climate models (RCMs). This is especially the case at a regional level, where the grid resolution of the models is too coarse to accurately resolve atmospheric processes, and the effects of topography and local climatology on the fine-scale spatial

structure of rainfall statistics (i.e., rainfall occurrence, amount and frequency of extremes; see sections 1 and 4).

Since accurate precipitation estimates are of increased importance for determining hydrological budgets, the availability of water resources in space and time, and flood risks, several statistical correction approaches (usually referred to as bias correction procedures) have been developed [see e.g., *Johnson and Sharma*, 2011; *Gudmundsson et al.*, 2012; *Lafon et al.*, 2013; *Langousis et al.*, 2016b], with distribution mapping being identified as the most suitable one for hydrologic applications [see e.g., *Piani et al.*, 2010; *Teutschbein and Seibert*, 2012, 2013]. Yet its implementation based on empirical distributions derived from control samples (referred to as nonparametric or empirical distribution mapping), makes the method's performance sensitive to sample length variations, the presence of outliers, the spatial resolution of CM results, and may lead to significant biases, especially when focus is on extreme rainfall estimation; see section 4.

A promising alternative is the use of parametric approaches, where Q-Q correction is conducted based on theoretical distribution models fitted to historical and CM simulated rainfall data [see *Piani et al.*, 2010; *Teutschbein and Seibert*, 2012; *Lafon et al.*, 2013; *Gutjahr and Heinemann*, 2013]. When properly selected and fitted, theoretical distribution models: (a) allow for more robust rainfall estimates, with approximate validity also beyond the range of the historical data [see *Piani et al.*, 2010; *Lafon et al.*, 2013; *Langousis et al.*, 2016b], and (b) reduce the computational effort associated with regional frequency analysis of extreme rainfall, as spatial interpolation is done in terms of distribution parameters, rather than empirical quantiles; see section 1. Also, proper interpolation of distribution parameters at high spatial resolutions allows for simultaneous bias correction and statistical downscaling of climate model results (i.e., corresponding to areal averages inside grid cells) to spatial scales resolved by the observational data (e.g., point rainfall, when using rain-gauge measurements, as in the present study), with subsequent modeling of small-scale rainfall variability.

In this study, we used a two-component theoretical distribution model (i.e., a generalized Pareto (GP) model for rainfall intensities above a specified threshold u^* , and an exponential model for lower rainrates) to propose and test a parametric approach for simultaneous bias correction and spatial rainfall downscaling, suited for regional frequency analysis. The latter was implemented by proper interpolation of the corresponding distribution parameters on a user-defined high-resolution grid, using kriging for uncertain data (KUD). Testing was conducted on the basis of an extended real-world case study in the island of Sardinia (Italy), for the 58-year period 1951–2008 (see section 2), where: (a) we applied both nonparametric and suggested parametric Q-Q correction approaches to rainfall products from four different climate models (i.e., KNMI, MPI, C4I, and SMHE), and different combinations of nonoverlapping calibration and validation periods, (b) assessed the relative performance of the two methodologies in reproducing the mean annual rainfall depth and extreme rainfall estimates for different exceedance probability (or equivalently return period) levels, and c) studied the sensitivity of each approach to the characteristics of the calibration period (including its length), the density of the raingauge network, and the climate model used. To the best of our knowledge, this is the first time that an extensive comparison study of parametric and nonparametric approaches for Q-Q correction of CM results is conducted on a fine resolution grid (i.e., ~ 1 km).

The obtained results indicate that while neither approach can perfectly reproduce the historical rainfall statistics based on CM data, parametric Q-Q correction is more efficient in modeling the effects of topography and local climatology on the magnitude, general tendencies, and high-resolution spatial structure of rainfall statistics (see section 4). This is especially the case for extreme rainfall, where use of a GP distribution model to describe the upper tail of rainfall observations and the robustness of the multiple threshold method (MTM) used for parameter estimation, allow for accurate rainfall intensity estimates at high return period levels, with reduced sensitivity to the length of the calibration period and the climate model used. These important attributes of the suggested parametric Q-Q correction procedure can be useful in several applications requiring accurate and robust estimates of precipitation at spatiotemporal resolutions suitable to run hydrologic models (e.g., assessment of the quality and availability of water resources in space and time and extreme flood estimation), and it is expected to significantly improve assessment of hydrologic risks and water management practices at a regional level, based on climate model results. Future research could potentially focus on extensions/refinements of the suggested parametric approach to include additional predictor variables (e.g., surface elevation, orientation, and distance from the coast) to condition KUD interpolation of distribution parameters, as well as applications to future periods, and to other hydrometeorologic variables such as near-surface temperature and wind speed.

Acknowledgments

The work of Antonios Mamalakis was supported by LIFE (Linked Institutions for Future Earth) funded under NSF's Science Across Virtual Institutes (SAVI) program (NSF grant EAR-1242458). The work of Andreas Langousis was supported by the Onassis Foundation under the "Special Grant and Support Program for Scholars' Association Members." The work conducted by Roberto Deidda was funded under the Sardinian Regional Law 7/2007 (funding call 2013). CRS4 highly acknowledges the contribution of the Sardinian regional authorities. The daily rainfall measurements used in this study are freely available in .pdf format at <http://www.regione.sardegna.it/j/v/25?s=205270&v=2&c=5650&t=1>. A digital copy of the recordings may be requested from the Hydrological Survey Agency of the Sardinia Region (<http://www.sar.sardegna.it/contatti/form.asp>; a fee applies). The climate model data used are freely available at: http://ensemblesrt3.dmi.dk/extended_table.html. The Authors would like to explicitly thank the Associate Editor and three anonymous reviewers for their very constructive comments and suggestions.

References

- Alexander, L. V., et al. (2006), Global observed changes in daily climate extremes of temperature and precipitation, *J. Geophys. Res.*, *111*, D05109, doi:10.1029/2005JD006290.
- Annan, J. D., J. C. Hargreaves, and K. Tachiiri (2011), On the observational assessment of climate model performance, *Geophys. Res. Lett.*, *38*, L24702, doi:10.1029/2011GL049812.
- Argüeso, D., J. P. Evans, and L. Fita (2013), Precipitation bias correction of very high resolution regional climate models, *Hydrol. Earth Syst. Sci.*, *17*, 4379–4388, doi:10.5194/hess-17-4379-2013.
- Baguis, P., E. Roulin, P. Willems, and V. Ntegeka (2009), Climate change scenarios for precipitation and potential evapotranspiration over central Belgium, *Theor. Appl. Clim.*, *99*(3–4), 273–286, doi:10.1007/s00704-009-0146-5.
- Balkema, A. A., and L. de Haan (1974), Residual lifetime at great age, *Ann. Probab.*, *2*, 792–804.
- Bastola, S., C. Murphy, and J. Sweeney (2011), The role of hydrological modelling uncertainties in climate change impact assessments of Irish river catchments, *Adv. Water Resour.*, *34*(5), 562–576.
- Bates, B. C., S. P. Charles, and J. P. Hughes (1998), Stochastic downscaling of numerical climate model simulations, *Environ. Model. Software*, *13*(3–4), 325–331.
- Busuioc, A., F. Giorgi, X. Bi, and M. Ionita (2006), Comparison of regional climate model and statistical downscaling simulations of different winter precipitation change scenarios over Romania, *Theor. Appl. Clim.*, *86*(1–4), 101–123.
- Caesar, J., L. Alexander, and R. Vose (2006), Large-scale changes in observed daily maximum and minimum temperatures: Creation and analysis of a new gridded data set, *J. Geophys. Res.*, *111*, D05101, doi:10.1029/2005JD006280.
- Camici, S., L. Brocca, F. Melone, and T. Moramarco (2014), Impact of climate change on flood frequency using different climate models and downscaling approaches, *J. Hydrol. Eng.*, *19*(8), 04014002-1-04014002-15, doi:10.1061/(ASCE)HE.1943-5584.0000959.
- Charles, S. P., B. C. Bates, P. H. Whetton, and J. P. Hughes (1999a), Validation of downscaling models for changed climate conditions: Case study of southwestern Australia, *Clim. Res.*, *12*, 1–14.
- Chen, C., J. O. Haerter, S. Hagemann, and C. Piani (2011), On the contribution of statistical bias correction to the uncertainty in the projected hydrological cycle, *Geophys. Res. Lett.*, *38*, L20403, doi:10.1029/2011GL049318.
- Coles, S. (2001), *An Introduction to Statistical Modeling of Extreme Values*, Springer, London.
- Cressie, N. (1985), Fitting variogram models by weighted least squares, *Math. Geol.*, *17*(5), 563–586.
- Deidda, R. (2010), A multiple threshold method for fitting the generalized Pareto distribution to rainfall time series, *Hydrol. Earth Syst. Sci.*, *14*(12), 2559–2575.
- Deidda, R., and M. Puliga (2006), Sensitivity of goodness-of-fit statistics to rainfall data rounding off, *Phys. Chem. Earth*, *31*(18), 1240–1251.
- Deidda, R., and M. Puliga (2009), Performances of some parameter estimators of the generalized Pareto distribution over rounded-off samples, *Phys. Chem. Earth*, *34*, 626–634.
- Deidda, R., M. Marrocu, G. Caroletti, G. Pusceddu, A. Langousis, V. Lucarini, M. Puliga, and A. Speranza (2013), Regional climate models' performance in representing precipitation and temperature over selected Mediterranean areas, *Hydrol. Earth Syst. Sci.*, *17*, 5041–5059, doi:10.5194/hess-17-5041-2013.
- de Marsily, G. (1986), *Quantitative Hydrogeology: Groundwater Hydrology for Engineers*, Academic, Orlando, Fla.
- Dentoni, M., R. Deidda, C. Paniconi, K. Qahman, and G. Lecca (2015), A simulation/optimization study to assess seawater intrusion management strategies for the Gaza Strip coastal aquifer (Palestine), *Hydrogeol. J.*, *23*, 249–264, doi:10.1007/s10040-014-1214-1.
- Déqué, M. (2007), Frequency of precipitation and temperature extremes over France in an anthropogenic scenario: Model results and statistical correction according to observed values, *Global Planet. Change*, *57*, 16–26, doi:10.1016/j.gloplacha.2006.11.030.
- Déqué, M., D. P. Rowell, D. Lüthi, F. Giorgi, J. H. Christensen, B. Rockel, D. Jacob, E. Kjellström, M. de Castro, and B. van den Hurk (2007), An intercomparison of regional climate simulations for Europe: Assessing uncertainties in model projections, *Clim. Change*, *81*(S1), 53–70.
- Dibike, Y. B., P. Gachon, A. St-Hilaire, T. B. M. J. Ouara, and Van T.-V. Nguyen (2008), Uncertainty analysis of statistically downscaled temperature and precipitation regimes in Northern Canada, *Theor. Appl. Clim.*, *91*(1–4), 149–170.
- Di Luca, A., R. de Elia, and R. Laprise (2011), Potential for added value in precipitation simulated by high-resolution nested Regional Climate Models and observations, *Clim. Dyn.*, *38*, 1229–1247, doi:10.1007/s00382-011-1068-3.
- Durman, C. F., J. M. Gregory, D. C. Hassell, R. G. Jones, and J. M. Murphy (2001), A comparison of extreme European daily precipitation simulated by a global and a regional climate model for present and future climates, *Q. J. R. Meteorol. Soc.*, *127*, 1005–1015.
- Evans, J. P., and M. F. McCabe (2013), Effect of model resolution on a regional climate model simulation over Southeast Australia, *Clim. Res.*, *56*, 131–145.
- Fatichi, S., V. Y. Ivanov, A. Paschalis, N. Peleg, P. Molnar, S. Rimkus, J. Kim, P. Burlando, and E. Caporali (2016), Uncertainty partition challenges the predictability of vital details of climate change, *Earth's Future*, *4*, 240–251, doi:10.1002/2015EF000336.
- Foley, A. M. (2010), Uncertainty in regional climate modelling: A review, *Prog. Phys. Geogr.*, *34*, 647–670, doi:10.1177/0309133310375654.
- Fowler, H. J., S. Blenkinsop, and C. Tebaldi (2007), Linking climate change modelling to impacts studies: Recent advances in downscaling techniques for hydrological modelling, *Int. J. Climatol.*, *27*, 1547–1578, doi:10.1002/joc.1556.
- Furcolo, P., A. Pelosi, and F. Rossi (2016), Statistical identification of orographic effects in the regional analysis of extreme rainfall, *Hydrol. Processes*, *30*, 1342–1353, doi:10.1002/hyp.10719.
- Gagnon, P., and A. N. Rousseau (2013), Stochastic spatial disaggregation of extreme precipitation to validate a Regional Climate Model and to evaluate climate change impacts over a small watershed, *Hydrol. Earth Syst. Sci. Discuss.*, *10*, 8167–8195, doi:10.5194/hessd-10-8167-2013.
- Giorgi, F., and R. Francisco (2000), Uncertainties in regional climate change prediction: A regional analysis of ensemble simulations with the HADCM2 coupled AOGCM, *Clim. Dyn.*, *16*, 169–182.
- Gleckler, P. J., K. E. Taylor, and C. Doutriaux (2008), Performance metrics for climate models, *J. Geophys. Res.*, *113*, D06104, doi:10.1029/2007JD008972.
- Greenwood, J. A., J. M. Landwehr, N. C. Matalas, and J. R. Wallis (1979), Probability weighted moments: Definition and relation to parameters of several distributions expressible in inverse form, *Water Resour. Res.*, *15*(5), 1049–1054.
- Gudmundsson, L., J. B. Bremnes, J. E. Haugen, and T. Engen-Skaugen (2012), Technical Note: Downscaling RCM precipitation to the station scale using statistical transformations—A comparison of methods, *Hydrol. Earth Syst. Sci.*, *16*, 3383–3390, doi:10.5194/hess-16-3383-2012.
- Gutjahr, O., and G. Heinemann (2013), Comparing precipitation bias correction methods for high-resolution regional climate simulations using COSMO-CLM, *Theor. Appl. Climatol.*, *114*, 511–529, doi:10.1007/s00704-013-0834-z.
- Gutmann, E., T. Pruitt, M. P. Clark, L. Brekke, J. R. Arnold, D. A. Raff, and R. M. Rasmussen (2014), An intercomparison of statistical downscaling methods used for water resource assessments in the United States, *Water Resour. Res.*, *50*, 7167–7186, doi:10.1002/2014WR015559.

- Hasson, S., V. Lucarini, and S. Pascale (2013), Hydrological cycle over South and Southeast Asian river basins as simulated by PCMDI/CMIP3 experiments, *Earth Syst. Dyn.*, *4*, 199–217, doi:10.5194/esd-4-199-2013.
- Hasson, S., V. Lucarini, S. Pascale, and J. Böhner (2014), Seasonality of the hydrological cycle in major South and Southeast Asian river basins as simulated by PCMDI/CMIP3 experiments, *Earth Syst. Dyn.*, *5*, 67–87, doi:10.5194/esd-5-67-2014.
- Herrmann, F., N. Baghdadi, M. Blaschek, R. Deidda, R. Duttman, I. La Jeunesse, H. Sellami, H. Vereecken, and F. Wendland (2016), Simulation of future groundwater recharge using a climate model ensemble and SAR-image based soil parameter distributions—A case study in an intensively-used Mediterranean catchment, *Sci. Total Environ.*, *543*, 889–905, doi:10.1016/j.scitotenv.2015.07.036.
- Hewitson, B. C., and R. G. Crane (2005), Gridded area-averaged daily precipitation via conditional interpolation, *J. Clim.*, *18*, 41–57.
- Hofstra, N., M. Haylock, M. New, P. Jones, and C. Frei (2008), Comparison of six methods for the interpolation of daily, European climate data, *J. Geophys. Res.*, *113*, D21110, doi:10.1029/2008JD010100.
- Hosking, J. R. M. (1990), L-moments: Analysis and estimation of distributions using linear combinations of order statistics, *J. R. Stat. Soc. Ser. B*, *52*, 105–124.
- Hosking, J. R. M. (1992), Moment or L moments? An example comparing two measures of distributional shape, *Am. Stat.*, *46*(3), 186–189.
- Hosking, J. R. M., and J. R. Wallis (1987), Parameter and quantile estimation for the generalized Pareto distribution, *Technometrics*, *29*, 339–349.
- Hosking, J. R. M., and R. Wallis (1997), *Regional Frequency Analysis: An Approach Based on L-moments*, Cambridge Univ. Press, Cambridge, U. K.
- Hosking, J. R. M., J. R. Wallis, and E. F. Wood (1985), Estimation of the generalized extreme-value distribution by the method of probability-weighted moments, *Technometrics*, *27*(3), 251–261.
- IPCC (2001), *Climate Change. The Scientific Basis*, 881 pp., Cambridge, U. K.
- IPCC (2007), Summary for policymakers, in *Climate Change 2007: The Physical Science Basis. Contribution of Working Group I to the Fourth Assessment Report of the Intergovernmental Panel on Climate Change*, edited by S. Solomon et al., Cambridge Univ. Press, Cambridge, U. K.
- Johnson, F., and A. Sharma (2009), Measurement of GCM skill in predicting variables relevant for hydroclimatological assessments, *J. Clim.*, *22*, 4373–4382, doi:10.1175/2009JCLI2681.1.
- Johnson, F., and A. Sharma (2011), Accounting for interannual variability: A comparison of options for water resources climate change impact assessments, *Water Resour. Res.*, *47*, W04508, doi:10.1029/2010WR009272.
- Kiktev, D., J. Caesar, L. V. Alexander, H. Shiogama, and M. Collier (2007), Comparison of observed and multimodeled trends in annual extremes of temperature and precipitation, *Geophys. Res. Lett.*, *34*, L17070, doi:10.1029/2007GL029539.
- King, A. D., L. V. Alexander, and M. G. Donat (2013), The efficacy of using gridded data to examine extreme rainfall characteristics: A case study for Australia, *Int. J. Climatol.*, *33*, 2376–2387, doi:10.1002/joc.3588.
- Kitanidis, P. K. (1993), Geostatistics, in *Handbook of Hydrology*, edited by D. R. Maidment, McGraw-Hill, New York.
- Kitanidis, P. K. (1997), *Introduction to Geostatistics: Applications to Hydrogeology*, Cambridge Univ. Press, New York.
- Kjellström, E., F. Boberg, M. Castro, J. H. Christensen, G. Nikulin, and E. Sánchez (2010), Daily and monthly temperature and precipitation statistics as performance indicators for regional climate models, *Clim. Res.*, *44*, 135–150, doi:10.3354/cr00932.
- Kleinn, J., C. Frei, J. Gurtz, D. Lüthi, P. L. Vidale, and C. Schär (2005), Hydrologic simulations in the Rhine basin driven by a regional climate model, *J. Geophys. Res.*, *110*, D04102, doi:10.1029/2004jd005143.
- Klemeš, V. (1986), Operational testing of hydrological simulation models/Vérification, en conditions réelles, des modèles de simulation hydrologique, *Hydrolog. Sci. J.*, *31*, 13–24, doi:10.1080/02626668609491024.
- Koutsoyiannis, D., and A. Langousis (2011), Precipitation, in *Treaties on Water Sciences: Hydrology*, vol. 2, edited by P. Wilderer and S. Uhlenbrook, pp. 27–78, Academic, Oxford, U. K.
- Krige, D. G. (1951), A statistical approach to some basic mine valuation problems on the Witwatersrand, *J. Chem. Metall. Min. Soc. S. Afr.*, *52*, 119–139.
- Krige, D. G. (1966), Two-dimensional weighted moving average trend surfaces for ore evaluation, *J. S. Afr. Inst. Min. Metall.*, *66*, 13–38.
- Lafon, T., S. Dadson, G. Buys, and C. Prudhomme (2013), Bias correction of daily precipitation simulated by a regional climate model: A comparison of methods, *Int. J. Climatol.*, *33*, 1367–1381, doi:10.1002/joc.3518.
- La Jeunesse, I., et al. (2016), Is climate change a threat for water uses in the Mediterranean region? Results from a survey at local scale, *Sci. Total Environ.*, *543*, 981–996, doi:10.1016/j.scitotenv.2015.04.062.
- La Jeunesse, I., C. Cirelli, H. Sellami, D. Aubin, R. Deidda, and N. Baghdadi (2015), Is the governance of the Thau coastal lagoon ready to face climate change impacts?, *Ocean Coastal Manage.*, *118*, 234–246, doi:10.1016/j.ocecoaman.2015.05.014.
- Langousis, A., and V. Kaleris (2013), Theoretical framework to estimate spatial rainfall averages conditional on river discharges and point rainfall measurements from a single location: An application to western Greece, *Hydrol. Earth Syst. Sci.*, *17*, 1241–1263, doi:10.5194/hess-17-1241-2013.
- Langousis, A., and V. Kaleris (2014), Statistical framework to simulate daily rainfall series conditional on upper-air predictor variables, *Water Resour. Res.*, *50*, 3907–3932, doi:10.1002/2013WR014936.
- Langousis, A., and D. Veneziano (2007), intensity-duration-frequency curves from scaling representations of rainfall, *Water Resour. Res.*, *43*, W02422, doi:10.1029/2006WR005245.
- Langousis, A., D. Veneziano, P. Furcolo, and C. Lepore (2009), Multifractal rainfall extremes: Theoretical analysis and practical estimation, *Chaos Solitons Fractals*, *39*, 1182–1194, doi:10.1016/j.chaos.2007.06.004.
- Langousis, A., A. A. Carsteanu, and R. Deidda (2013), A simple approximation to multifractal rainfall maxima using a generalized extreme value distribution model, *Stochastic Environ. Res. Risk Assess.*, *27*, 1525–1531, doi:10.1007/s00477-013-0687-0.
- Langousis, A., A. Mamalakis, M. Puliga, and R. Deidda (2016a), Threshold detection for the generalized Pareto distribution: Review of representative methods and application to the NOAA NCDC daily rainfall database, *Water Resour. Res.*, *52*, 2659–2681, doi:10.1002/2015WR018502.
- Langousis, A., A. Mamalakis, R. Deidda, and M. Marrocu (2016b), Assessing the relative effectiveness of statistical downscaling and distribution mapping in reproducing rainfall statistics based on climate model results, *Water Resour. Res.*, *52*, 471–494, doi:10.1002/2015WR017556.
- Laprise, R., R. de Elia, D. Caya, S. Biner, P. Lucas-Picher, E. Diaconescu, M. Leduc, A. Alexandru, and L. Separovic (2008), Challenging some tenets of regional climate modelling, *Meteorol. Atmos. Phys.*, *100*, 3–22, doi:10.1007/s00703-008-0292-9.
- Leadbetter, M. R. (1991), On a basis for “peak over threshold” modeling, *Stat. Probab. Lett.*, *12*, 357–362.
- Leadbetter, M. R., G. Lindgren, and H. Rootzen (1983), *Extremes and Related Properties of Random Sequences and Series*, Springer, New York.
- Leander, R., and T. A. Buishand (2007), Resampling of regional climate model output for the simulation of extreme river flows, *J. Hydrol.*, *332*(3–4), 487–496.
- Leander, R., T. A. Buishand, B. J. J. M. van den Hurk, and M. J. M. de Wit (2008), Estimated changes in flood quantiles of the river Meuse from resampling of regional climate model output, *J. Hydrol.*, *351*(3–4), 331–343.

- Lucarini, V., R. Danihlik, I. Kriegerova, and A. Speranza (2007), Does the Danube exist? Versions of reality given by various regional climate models and climatological data sets, *J. Geophys. Res.*, *112*, D13103, doi:10.1029/2006JD008360.
- Lucarini, V., D. Faranda, A. C. G. M. M. de Freitas, J. M. M. de Freitas, M. Holland, T. Kuna, M. Nicol, M. Todd, and S. Vaienti (2016), *Extremes and recurrence in dynamical systems*, 304 pp., John Wiley, Hoboken, N. J.
- Majone, B., F. Villa, R. Deidda, and A. Bellin (2016), Impact of climate change and water use policies on hydropower potential in the south-eastern Alpine region, *Sci. Total Environ.*, *543*, 965–980, doi:10.1016/j.scitotenv.2015.05.009.
- Mao, G., S. Vogl, P. Laux, S. Wagner, and H. Kunstmann (2015), Stochastic bias correction of dynamically downscaled precipitation fields for Germany through Copula-based integration of gridded observation data, *Hydrol. Earth Syst. Sci.*, *19*, 1787–1806, doi:10.5194/hess-19-1787-2015.
- Maraun, D., et al. (2010), Precipitation downscaling under climate change: Recent developments to bridge the gap between dynamical models and the end user, *Rev. Geophys.*, *48*, RG3003, doi:10.1029/2009RG000314.
- Martins, E. S., and J. R. Stedinger (2001a), Historical information in a generalized maximum likelihood framework with partial duration and annual maximum series, *Water Resour. Res.*, *37*(10), 2559–2567.
- Martins, E. S., and J. R. Stedinger (2001b), Generalized maximum likelihood Pareto-Poisson estimators for partial duration series, *Water Resour. Res.*, *37*(10), 2551–2557.
- Mascaro, G., R. Deidda, and M. Hellies (2013), On the nature of rainfall intermittency as revealed by different metrics and sampling approaches, *Hydrol. Earth Syst. Sci.*, *17*, 1–15.
- Mascaro, G., D. D. White, P. Westerhoff, and N. Bliss (2015), Performance of the CORDEX-Africa regional climate simulations in representing the hydrological cycle of the Niger River basin, *J. Geophys. Res. Atmos.*, *120*, 12,425–12,444, doi:10.1002/2015JD023905.
- Matheron, G. (1971), *The Theory of Regionalized Variables and Its Applications*, 211 pp., Cah. du Cent. de Morphol. Math., École de Mines, Paris.
- Maurer, E. P., and H. G. Hidalgo (2008), Utility of daily vs. monthly large-scale climate data: An intercomparison of two statistical downscaling methods, *Hydrol. Earth Syst. Sci.*, *12*(2), 551–563, doi:10.5194/hess-12-551-2008.
- Maurer, E. P., D. L. Ficklin, and W. Wang (2016), Technical note: The impact of spatial scale in bias correction of climate model output for hydrologic impact studies, *Hydrol. Earth Syst. Sci.*, *20*(2), 685–696, doi:10.5194/hess-20-685-2016.
- Mazzetti, C., and E. Todini (2009), Combining weather radar and raingauge data for hydrologic applications, in *Flood Risk Management: Research and Practice*, edited by P. Samuels et al., Taylor and Francis, London.
- Mearns, L. O., F. Giorgi, L. McDaniel, and C. Shields (1995), Analysis of daily variability of precipitation in a nested regional climate model: Comparison with observations and doubled CO₂ results, *Global Planet. Change*, *10*, 55–78.
- Mehrotra, R., and A. Sharma (2016), A multivariate quantile-matching bias correction approach with auto- and cross-dependence across multiple time scales: implications for downscaling, *J. Clim.*, *29*, 3519–3539, doi: 10.1175/JCLI-D-15-0356.1.
- Michelangeli, P. A., M. Vrac, and H. Loukos (2009), Probabilistic downscaling approaches: Application to wind cumulative distribution functions, *Geophys. Res. Lett.*, *36*, L11708, doi:10.1029/2009GL038401.
- Moral, F. J. (2009), Comparison of different geostatistical approaches to map climate variables: Application to precipitation, *Int. J. Climatol.*, *30*, 620–631, doi:10.1002/joc.1913.
- Palatella, L., M. M. Miglietta, P. Paradisi, and P. Lionello (2010), Climate change assessment for Mediterranean agricultural areas by statistical downscaling, *Nat. Hazards Earth Syst. Sci.*, *10*, 1647–1661.
- Pan, Z., J. H. Christensen, R. W. Arritt, W. J. Gutowsky, E. S. Takle, and F. Otieno (2001), Evaluation of uncertainties in regional climate change simulations, *J. Geophys. Res.*, *106*(D16), 735–751.
- Papalexiou, S. M., D. Koutsoyiannis, and C. Makropoulos (2013), How extreme is extreme? An assessment of daily rainfall distribution tails, *Hydrol. Earth Syst. Sci.*, *17*(2), 851–862.
- Perkins, S., A. Pitman, N. Holbrook, and J. McAneney (2007), Evaluation of the AR4 climate models simulated daily maximum temperature, minimum temperature and precipitation over Australia using probability density functions, *J. Clim.*, *20*, 4356–4376.
- Piani, C., J. O. Haerter, and E. Coppola (2010), Statistical bias correction for daily precipitation in regional climate models over Europe, *Theor. Appl. Climatol.*, *99*(1), 187–192, doi:10.1007/s00704-009-0134-9.
- Pickands, J. (1975), Statistical inference using extreme order statistics, *Ann. Stat.*, *3*, 119–131.
- Piras, M., G. Mascaro, R. Deidda, and E. R. Vivoni (2014), Quantification of hydrologic impacts of climate change in a Mediterranean basin in Sardinia, Italy, through high-resolution simulations, *Hydrol. Earth Syst. Sci.*, *18*, 5201–5217, doi:10.5194/hess-18-5201-2014.
- Piras, M., G. Mascaro, R. Deidda, and E. R. Vivoni (2016), Impacts of climate change on precipitation and discharge extremes through the use of statistical downscaling approaches in a Mediterranean basin, *Sci. Total Environ.*, *543*, 952–964, doi:10.1016/j.scitotenv.2015.06.088.
- Prudhomme, C., N. Reynard, and S. Crooks (2002), Downscaling of global climate models for flood frequency analysis: Where are we now?, *Hydrol. Processes*, *16*, 1137–1150.
- Räisänen, J. (2006), How reliable are climate models?, *Tellus, Ser. A*, *59*, 2–29, doi:10.1111/j.1600-0870.2006.00211.x.
- Raje, D., and P. P. Mujumdar (2009), A conditional random field-based downscaling method for assessment of climate change impact on multisite daily precipitation in the Mahanadi basin, *Water Resour. Res.*, *45*, W10404, doi:10.1029/2008WR007487.
- Rojas, R., L. Feyen, A. Dosio, and D. Bavera (2011), Improving pan-European hydrological simulation of extreme events through statistical bias correction of RCM-driven climate simulations, *Hydrol. Earth Syst. Sci.*, *15*(8), 2599–2620.
- Salathé, E. P., Jr. (2003), Comparison of various precipitation downscaling methods for the simulation of streamflow in a rainshadow river basin, *Int. J. Climatol.*, *23*, 887–901, doi:10.1002/joc.922.
- Sennikovs, J., and U. Bethers (2009), Statistical downscaling method of regional climate model results for hydrological modelling, in *18th World IMACS Congress and MODSIM09 International Congress on Modelling and Simulation*, edited by R. S. Anderssen, R. D. Braddock, and L. T. H. Newham, pp. 3962–3968, Modell. and Simul. Soc. of Aust. [Available at <http://www.mssanz.org.au/modsim09/F12/kragt.pdf>].
- Serinaldi, F., and C. G. Kilsby (2014), Rainfall extremes: Toward reconciliation after the battle of distributions, *Water Resour. Res.*, *50*, 336–352, doi:10.1002/2013WR014211.
- Singh, V. P. (1992), *Elementary Hydrology*, Prentice-Hall, Upper Saddle River, N. J.
- Smiatek, G., H. Kunstmann, R. Knoche, and A. Marx (2009), Precipitation and temperature statistics in high-resolution regional climate models: Evaluation for the European Alps, *J. Geophys. Res.*, *114*, D19107, doi:10.1029/2008JD011353.
- Smith, J. A. (1993), Precipitation, in *Handbook of Applied Hydrology*, chap. 3, edited by A. A. Maidment, pp. 3.1–3.47, McGraw-Hill, New York.
- Smith, R. L. (1985), Maximum likelihood estimation in a class of non-regular cases, *Biometrika*, *72*, 67–90.
- Stahl, K., R. D. Moore, J. A. Floyer, M. G. Asplin, and I. G. McKendry (2006), Comparison of approaches for spatial interpolation of daily air temperature in a large region with complex topography and highly variable station density, *Agric. For. Meteorol.*, *139*, 224–236, doi: 10.1016/j.agrformet.2006.07.004.

- Stedinger, J. R., R. M. Vogel, and E. Foufoula-Georgiou (1993), Frequency analysis of extreme events, in *Handbook of Hydrology*, chap. 18, edited by D. A. Maidment, pp. 18-1–18-66, McGraw-Hill, New York.
- Stoll, S., H. J. Hendricks Franssen, M. Butts, and W. Kinzelbach (2011), Analysis of the impact of climate change on groundwater related hydrological fluxes: A multi-model approach including different downscaling methods, *Hydrol. Earth Syst. Sci.*, *15*(1), 21–38.
- Sulis, M., C. Paniconi, M. Marrocu, D. Huard, and D. Chaumont (2012), Hydrologic response to multimodel climate output using a physically based model of groundwater/surface water interactions, *Water Resour. Res.*, *48*, W12510, doi:10.1029/2012WR012304.
- Sun, F., M. L. Roderick, W. H. Lim, and G. D. Farquhar (2011), Hydroclimatic projections for the Murray–Darling Basin based on an ensemble derived from Intergovernmental Panel on Climate Change AR4 climate models, *Water Resour. Res.*, *47*, W00G02, doi:10.1029/2010WR009829.
- Teutschbein, C., and J. Seibert (2012), Bias correction of regional climate model simulations for hydrological climate-change impacts studies: Review and evaluation of different methods, *J. Hydrol.*, *456–457*, 12–29.
- Teutschbein, C., and J. Seibert (2013), Is bias correction of regional climate model (RCM) simulations possible for non-stationary conditions?, *Hydrol. Earth Syst. Sci.*, *17*, 5061–5077.
- Teutschbein, C., F. Wetterhall, and J. Seibert (2011), Evaluation of different downscaling techniques for hydrological climate-change impact studies at the catchment scale, *Clim. Dyn.*, *37*, 2087–2105, doi:10.1007/s00382-010-0979-8.
- Thiemeß, M. J., A. Gobiet, and A. Leuprecht (2011), Empirical-statistical downscaling and error correction of daily precipitation from regional climate models, *Int. J. Climatol.*, *31*(10), 1530–1544, doi:10.1002/joc.2168.
- Trenberth, K. E., A. Dai, R. M. Rasmussen, and D. B. Parsons (2003), The changing character of precipitation, *Bull. Am. Meteorol. Soc.*, *84*, 1205–1217, doi:10.1175/BAMS-84-9-1205.
- Urrutia, R., and M. Vuille (2009), Climate change projections for the tropical Andes using a regional climate model: Temperature and precipitation simulations for the end of the 21st century, *J. Geophys. Res.*, *114*, D02108, doi:10.1029/2008JD011021.
- van Pelt, S. C., J. J. Beersma, T. A. Buishand, B. J. J. M. van den Hurk, and P. Kabat (2012), Future changes in extreme precipitation in the Rhine basin based on global and regional climate model simulations, *Hydrol. Earth Syst. Sci.*, *16*, 4517–4530, doi:10.5194/hess-16-4517-2012.
- Veneziano, D., and A. Langousis (2005), The areal reduction factor a multifractal analysis, *Water Resour. Res.*, *41*, W07008, doi:10.1029/2004WR003765.
- Veneziano, D., and S. Yoon (2013), Rainfall extremes, excesses, and intensity-duration-frequency curves: A unified asymptotic framework and new nonasymptotic results based on multifractal measures, *Water Resour. Res.*, *49*, 4320–4334, doi:10.1002/wrcr.20352.
- Veneziano, D., C. Lepore, A. Langousis, and P. Furcolo (2007), Marginal methods of intensity-duration-frequency estimation in scaling and nonscaling rainfall, *Water Resour. Res.*, *43*, W10418, doi:10.1029/2007WR006040.
- Veneziano, D., A. Langousis, and C. Lepore (2009), New asymptotic and preasymptotic results on rainfall maxima from multifractal theory, *Water Resour. Res.*, *45*, W11421, doi:10.1029/2009WR008257.
- Vicente-Serrano, S. M., M. A. Saz-Sánchez, and J. M. Cuadrat (2003), Comparative analysis of interpolation methods in the middle Ebro Valley (Spain): Application to annual precipitation and temperature, *Clim. Res.*, *24*, 161–180.
- von Storch, H., E. Zorita, and U. Cubasch (1993), Downscaling of global climate estimates to regional scales: An application to Iberian Rainfall in Wintertime, *J. Clim.*, *6*, 1161–1171.
- Vrac, M., P. Marbaix, D. Paillard, and P. Naveau (2007), Non-linear statistical downscaling of present and LGM precipitation and temperatures over Europe, *Clim. Past*, *3*, 669–682, doi:10.5194/cp-3-669-2007.
- Walsh, K. J. E., and J. L. McGregor (1995), January and July climate simulations over the Australian region using a limited area model, *J. Clim.*, *8*(10), 2387–2403.
- Wetterhall, F., A. Bárdossy, D. Chen, S. Halldin, and C.-Y. Xu (2009), Statistical downscaling of daily precipitation over Sweden using GCM output, *Theor. Appl. Climatol.*, *96*(1-2), 95–103, doi:10.1007/s00704-008-0038-0.
- Wilby, R. L. (2010), Evaluating climate model outputs for hydrological applications, *Hydrolog. Sci. J.*, *55*, 1090–1093.
- Wilby, R. L., and I. Harris (2006), A framework for assessing uncertainties in climate change impacts: Low-flow scenarios for the River Thames, UK, *Water Resour. Res.*, *42*, W02419, doi:10.1029/2005WR004065.
- Willems, P., and M. Vrac (2011), Statistical precipitation downscaling for small-scale hydrological impact investigations of climate change, *J. Hydrol.*, *402*(3–4), 193–205, doi:10.1016/j.jhydrol.2011.02.030.
- Wood, A. W., L. R. Leung, V. Sridhar, and D. P. Lettenmaier (2004), Hydrologic implications of dynamical and statistical approaches to downscaling climate model outputs, *Clim. Change*, *62*(1–3), 189–216, doi:10.1023/B:CLIM.0000013685.99609.9e.